



INTERNATIONAL ATOMIC ENERGY AGENCY  
UNITED NATIONS EDUCATIONAL, SCIENTIFIC AND CULTURAL ORGANIZATION



INTERNATIONAL CENTRE FOR THEORETICAL PHYSICS  
34100 TRIESTE (ITALY) - P.O.B. 586 - MIRAMARE - STRADA COSTIERA 11 - TELEPHONE: 2240-1  
CABLE: CENTRATOM - TELEX 460392-1

II4.SMR/204 - 11

# ICTP WINTER COLLEGE ON ATOMIC AND MOLECULAR PHYSICS

TRIESTE , March 1987

WINTER COLLEGE ON  
ATOMIC AND MOLECULAR PHYSICS

(9 March - 3 April 1987)

(ANALYTICAL LASER SPECTROSCOPY 1)

Lasers as Atomizers &  
Laser Induced Breakdown Spectroscopy

N. OMENETTO  
Joint Research Centre  
Ispra (Va), Italy

## "ANALYTICAL LASER SPECTROSCOPY 1"

Lecturer : N. OMENETTO

Joint Research Centre  
Ispra (Va) , Italy

K. Laqua

Institut für Spektrochemie und angewandte Spektroskopie,  
Postfach 778, D-4600 Dortmund 1, Federal Republic of Germany

## VIII.

☆ Lasers as Atomizers

☆ Laser Induced Breakdown Spectroscopy

### 1. Introduction

In this article, laser as a source of thermal energy supplementing customary spectrochemical excitation sources will be treated. It is therefore necessary to first explain the properties of typical excitation sources. In optical spectrochemical analysis, chemical elements contained in a sample are determined with the help of their optical line spectra. This can only be done, if a representative part of a solid or liquid sample is first converted into atomic vapour. Free atoms can then either be determined with the help of their absorption spectra or, if suitably excited, with the help of their emission spectra. It is, of course, also possible to detect the elements with the help of ionized atoms either by atomic emission spectroscopy or by mass spectrometry.

The customary radiation sources can be divided into two groups, e.g. electrical radiation sources and non-electrical radiation sources. The former group comprises electrical arcs, sparks and discharges under reduced pressure or in vacuum. Evaporation of sample material and excitation are both effected by the same source. Electrically conducting samples can be analysed directly, whereas electrically non-conducting samples have to be suitably prepared e.g. by grinding them down and mixing with conducting material. It is well known that the evaporation and excitation in electrical radiation sources can be

strongly influenced by the chemical and physical properties of the sample. Great care has therefore to be exercised to avoid systematic analytical errors.

The second group of radiation sources can best be called 'plasmas'. They comprise chemically produced plasmas, e.g. flames and electrically produced plasmas, e.g. microwave induced plasmas, induction coupled plasmas, etc. Commonly, the sample has to be converted into an aerosol which then is introduced into the plasma and excited. Solid materials are usually first dissolved, but direct production of an aerosol from such substances is also possible.

For local analysis, several methods have been described in literature. With electrical radiation sources, spatial resolution can be improved by using a pointed counter electrode, preferably in connection with a confinement of the surface area which can be attacked by the discharge. With non-conducting surfaces, a local analysis can only be performed indirectly by first mechanically removing the respective part of the sample and subsequently analysing it by a standard method.

Soon after the first realization of a Ruby laser in 1960 by Maiman<sup>1</sup> in 1962, a 'Laser Microprobe' designed for local analysis was described and introduced into analytical routine by Brech and Cross<sup>2</sup>. Understandably, due to lack of fast and powerful methods for local spectrochemical analysis, the first methods of application of laser centered around this special analytical technique. Since then, the scope of application has widened considerably and now comprises surface, micro- and macro-analysis as well. The particular properties of laser as excitation source in optical

and mass spectroscopy rest upon the fact that powerful radiation is emitted with a very small angle of divergence. It can therefore, be concentrated into a very small spot at the focus of the lens. The irradiance of material in this spot may be sufficiently high for vaporizing material for spectral analysis. This applies to all kinds of materials irrespective of their electrical properties. The vapour may have such a high temperature, depending on the mode of operation of the laser system, that the characteristic radiation of the pertaining atoms is excited or the atoms are ionized. It is also possible to further excite the laser-produced vapour plume by several means. Both methods have their relative merits. The principle of operation of a laser source for optical spectroscopy can best be understood with the help of Fig. 1, which is a semi-schematic representation of a commercial instrument. It consists basically of the laser including the Q-switch, a microscope for aligning the sample and focusing the laser radiation on the surface and an electrode system for auxiliary cross spark excitation. The instrument as shown, is primarily thought for optical emission spectroscopy in local analysis, but with some alterations, its applicability could be extended. A general survey of the analytical facilities obtainable with the help of laser atomizers is given in Fig. 2. A large number of research papers dealing with principles and applications of laser atomizers have been published. They are reviewed in articles by Scott and Strasheim<sup>3</sup> (150 references), Laqua<sup>4</sup> (113 references), Petukh and Yankovskii<sup>5</sup> (219 references). The book by Moenke and Moenke-Blankenburg<sup>6</sup> should also be consulted. An assessment of quantitative analytical possibilities is given by Van Deijck, Balke and Maessen<sup>7</sup>. Other more recent publications are the following<sup>8-60</sup>. Laser-induced formation of ions for mass spectrometry has first been described by Honig and Woolston<sup>61</sup>

in 1963. Since then, numerous reports on this subject have been published. The most recent, thorough review is that by Concemius and Capellen<sup>62</sup> (462, references). In addition, the new work by Jansen and Witmer<sup>63,64</sup> should be mentioned demonstrating the present state of the art. The history of high resolution laser microprobe mass spectrometry has been dealt with by Denoyer, Van Grieken, Adams and Natusch<sup>65</sup> who then describe in detail, a commercial instrument for this purpose, based on the work by Hillenkamp, Kauffmann, Nitsche and Unsöld<sup>66</sup>.

## 2. Lasers as used for Atomization

Some lasers suitable for atomization of solid samples and their operation ranges are listed in Table 1. Optically pumped as well as electrically excited configurations are used. Liquid lasers, although listed, have hardly been employed. By far the widest application have found the solid-state lasers, but it can be expected that excimer lasers, especially rare gas halogen lasers may have a future. For particulars concerning the latter, the reader is advised to consult for instance, the report by Hutchinson<sup>67</sup>.

With solid-state lasers, a wide range of output energy and power will be available depending on the size of the laser rod and on the pumping system. Rod lengths from 15 to 150 mm are typical with diameters ranging from 5 to 15 mm. The output energy may be between a few tenths of a joule and about 5 joule, but applications with considerably higher energy have been reported. Typical properties of ruby as active medium are the following: radiation in the visible region (0.6943  $\mu\text{m}$ ), good heat conductivity, comparatively high threshold energy, small angles of divergence with high quality rods. Glass rods doped with Nd have

lower thresholds, radiate in the near infrared (1.06  $\mu\text{m}$ ) which may be advantageous for the analysis of dielectric materials, and are thermally more sensitive than ruby rods. Laser with rods fabricated from yttrium aluminium garnet (YAG) doped with neodymium permit very low lasing thresholds and therefore, are very suitable for higher repetition rates. Their peak power capability however, is more restricted than that of the other two.

In the free running operation mode, optically pumped lasers, once threshold is passed, radiate in a random sequence of single pulses called spikes which may have powers of a few kW. An emission of this kind is indicated in Fig. 2. For operation of the laser system in a Q-switched mode, several types of Q-switches may find application. The simplest type of a Q-switch is a bleachable filter which may either be solid or liquid. With such switches, one to several spikes per pumping cycle can be produced possessing powers of up to several MW. It should be mentioned, however, that this Q-switch cannot be externally triggered, a property which may be desirable for certain applications. Kerr cells or Pockels cells, very common with other high power laser operation, are also used in analytical practice. Rotating slotted disks, mirrors or prisms as Q-switches permit the operation with analytical properties lying between those of the free running and the fast Q-switched laser. Several types of acousto-optical Q-switches have been described, one of which produces a series of equidistant spikes for a considerable fraction of the pumping time, having powers of several 100 kW. This mode of operation is useful for some spectrochemical applications.

Very short, high power pulses can be obtained by mode locking, i.e. by forcing all modes in a laser oscillator to oscillate in phase, and with similar amplitudes in place of the random emission of spikes due to multimode oscillation. It has been claimed that mode-locked operation can be used with advantage with laser atomizers<sup>12</sup>.

### 3. Interactions of Laser with Solids

Radiation from a laser source is emitted with a very small angle of divergence (see Table 1). Its radiant intensity, that is, its radiant power per solid angle, can be very high, exceeding that of all other known sources. Focusing the laser radiation onto the target with the help of a lens or mirror can be very effective in producing small focal spots with corresponding high irradiance sufficient to vaporize any kind of material. By this interaction a crater is formed. Its dimensions depend on the area of the focal spot, on the mode of operation of the laser system, on the total energy delivered to the sample within the focal spot and on properties of the sample. The diameter of the crater does not coincide with the diameter of the focal area. In Fig. 3 the influence of some of the factors is demonstrated.

The mass of metal eroded by a free running laser is directly proportional to the fraction of absorbed energy and inversely proportional to the energy required to melt unit mass of the material<sup>17</sup>. Regarding the crater shape it can be said that the depth of the crater increases more rapidly with increasing energy than the diameter. At constant energy, the shape of the crater depends strongly on the mode of operation. An unswitched

laser emitting a large number of spikes of low power and low energy produces a rather deep crater in relation to its diameter due to the subsequent action of a large number of spikes following at very short intervals in which the material does not solidify. Usually, a wall of molten material is forming around the crater. Little overheating action takes place and the temperature of the vapour cloud is usually rather low with the consequence of very little emission of radiation. A considerable part of the material is not atomized either, but is ejected in the form of small liquid or recondensed particles. The fraction of vapour is of the order of 0.1%<sup>17</sup>. As this mode of operation is capable of producing the smallest craters (there is a threshold below which no evaporation takes place), it is most widely used in local analysis, but because of the poor radiation efficiency, additional excitation of the vapour cloud is compulsory.

The other extreme is the action of one single giant pulse as obtainable for instance, with the help of a Kerr or Pockels cell. With this mode of operation, very high power and power densities on the surface can be obtained. The result of the interaction with the surface is a very shallow crater with little or no molten residue. The diameter may be rather large. Because of the rapid overheating of sample material, the initial temperature of the vapour cloud expanding rapidly at initial velocities of a km per second or more, is high. From the appearance of the crater, it can be concluded that most of the removed material is atomized with only a very low fraction of molten or solid particles. The vapour cloud may radiate strongly. At the beginning, the radiation consists of a strong background due to the high pressure and rather broad

spectral lines. At a later stage, the background is reduced and the spectral lines become narrow; later still, band spectra are also detectable. The atomic radiation can directly be used for spectrochemical analysis at not too low concentrations.

With the help of bleachable filters it is possible to obtain several giant pulses at rather large intervals (distributed over most of the pumping time). The crater, due to the repeated attack of laser radiation on the sample surface, is deeper but otherwise of similar appearance because each giant pulse hits a rather cool surface. The spectra are very similar to those described above.

With Q-switch operation employing acousto-optical switches as described above, the dimensions of the crater and its shape are in between those obtainable with the free running laser and those obtainable by a sequence of giant spikes. Each of the 50 to 100 spikes interacts with a solid and rather cool surface. On the other hand, as compared to the free running laser, the power of the spikes is sufficiently high and consequently, the temperature of the vapour cloud, to effectively excite the atomic spectra of the respective elements, but with considerably less background.

This mode of operation should therefore be used for the direct analysis of solids in cases where high spatial resolution (very small crater) and high power of detection are not required. Regarding the erosion of material from solid surfaces, some more generalization can be made: With samples of low melting points, more material is removed, mostly in the form of liquid droplets, than predicted by theory. Crater diameters

can be less reliably forecast than crater depths. The reflection factor of the sample surface may also be of influence, but mainly at comparably low power. Special attention has to be paid if transparent or little absorbing materials have to be analysed, especially if they have high boiling temperatures, e.g. glasses. In these cases a high irradiance ( $10^9 \text{ W cm}^{-2}$ ) is necessary. Plastic material behaves similar to metals of low melting and boiling points. Comparably little atomic vapour is produced and the craters are rather large. Liquid materials can also be analysed but it is necessary to first convert them to solids by freezing. The same technique has been applied with success to biological samples, e.g. tissues.

On principle, gases could be handled in the same way although no such investigations have become known. They also could be analysed directly with the help of 'laser sparks', i.e. the direct dielectric breakdown in the respective gas caused by high power focused laser radiation. Analytical application of that technique apparently has also not been undertaken yet.

By strict control of the laser operating parameters, especially pumping energy and temperature, the reproducibility of the laser output can be high, whereas the resulting crater dimensions vary much more, typically 10% as in comparison to 1%. It has been shown that the reproducibility of crater dimensions can be significantly improved in cases where a face of a single crystal is attacked.

Vul'fson et al.<sup>10</sup> have investigated in detail the vaporization of material in a laser-produced plume, especially with the aim to ensure conformity of composition of the vapour with

the composition of the sample. For a more thorough treatment of the subject of interaction of laser radiation with solids, the reader is referred to the book by Ready<sup>69</sup>. Pertinent original papers are discussed for instance, in<sup>3,4,5,13,17,40,62</sup>.

#### 4. Atomic Absorption Spectroscopy using Laser Atomizers

The laser-produced vapour cloud contains a considerable proportion of neutral ground state atoms. Therefore, atomic absorption methods can be used to identify the elements producing these atoms. This has first been employed by Mossotti et al.<sup>70</sup>. The analytical signal must be separated from interfering emission signals which are usually also generated in the vapour cloud and should be corrected for nonspecific absorption in a standard manner. The former can be accomplished by choosing a suitable distance from the sample. This situation is illustrated in Fig. 4.

Basically, three different approaches for designing atomic absorption methods can be distinguished, namely those, in which the atomic absorption is directly observed, those in which the vapour cloud is in situ subjected to additional heating and those in which the vapour is transferred to the final atomization device, which may be a flame, a plasma or a furnace. Fig. 5 shows some of the possibilities.

Published work on atomic absorption analysis has been reviewed in<sup>4</sup>. A variety of techniques has been developed. As primary sources, continuous radiation from pulsed flash lamps as well as line radiation from pulsed hollow cathode lamps were used. Free running and Q-switched solid state lasers, continu-

ously emitting Ar<sup>+</sup> and pulsed CO<sub>2</sub> TEA lasers served as atomization devices. It is claimed that higher power of detection can be obtained by confining the vapour in a heated graphite cuvette. In two-step procedures, the final atomization is accomplished in a separate step which may substantially improve the power of detection. Of more recent work<sup>10,16,33,43,44,46,47</sup> it should be mentioned that Petukh et al.<sup>16</sup> used a spark cross discharge similar to that in emission work for the final atomization, Quentmeier et al.<sup>48,49</sup> an acousto-optical Q-switch for long-lasting vaporization and efficient atomization, Sumino et al.<sup>43</sup> combined laser ablation with electrothermal atomization. The same did Dittrich et al.<sup>44</sup>; Manabe and Piepmeier<sup>46</sup> used a dye laser for plume atomization combined with a pulsed HCL; Quillfeldt<sup>47</sup> compared AAS and AES and found similar analytical properties.

To sum up: Atomic absorption methods are basically single element determination methods and may therefore be of limited application possibility in cases where not enough material for several sequential determinations is available. Their limited dynamic concentration range may hamper the analysis of random samples of completely unknown composition.

#### 5. Atomic Fluorescence Spectroscopy using Laser Atomizers

These methods are closely related to AAS methods except that, due to the emission of radiation, a large concentration range is available from a single spectral line. From this point of view such methods are suitable for simultaneous multi-element determination (provided, simultaneous excitation can be effected). So far, only one application of AFS to laser-produced plume has been reported. Measures and Kwong<sup>52,58</sup> with

their 'Tablaser' atomized sample material with the help of Q-switched ruby radiation which was then excited at low pressure to resonance fluorescence by absorption of radiation from a nitrogen-laser pumped tuned dye-laser. At a spatial resolution of about 100  $\mu\text{m}$ , limits of detection of the order of 1  $\mu\text{g/g}$  or  $10^{-13}$  g respectively are claimed with the added advantage of relative freedom from matrix effects.

#### 6. Atomic Emission Spectroscopy using Laser Atomizers

The spectral character of optical emission spectra produced directly by laser atomizers differs from that of customary arc or spark discharges. It strongly depends on the power and mode of operation of the laser. Giant pulses produce a strong background and broad lines with, however, little or no self-reversal. On the other hand, unswitched operation with slow switches lead to spectra of lower continuous background and lines not quite as broad as in the case of resonance lines with pronounced self-reversal. As the latter are very often recommended as analytical lines, due care should be exercised by their use. Generally, the quality of the spectra is not as good as that of other spectrochemical light sources. In Fig. 6 some combinations for laser-optical emission spectroscopy are demonstrated.

Substances with a sufficiently high melting point are suited for direct analysis with the help of the spectrum as generated by the laser radiation impact. For some kinds of operation, especially if high spatial resolution and consequently, low power operation of the laser is necessary, a two-step process is the method of choice. i.e. the laser-produced

vapour plume is excited in an additional source. In this configuration, the primary radiation emerging from the vapour cloud is weak as compared to the one produced by the additional excitation which now mainly determines the spectral character of the radiation. Mode of operation of the laser, power and energy are again responsible for the crater dimensions, but of special importance are now also the transport of material into the excitation zone, the time of residence of the laser-produced vapour in this additional source and its thermodynamic properties.

The oldest and most popular method of additional excitation makes use of a spark discharge. This discharge takes place between two pointed electrodes, usually of pure graphite, and is fed from a charged condenser bank via suitable impedances (resistors and inductors). The energy stored in the condenser may be in the order of a joule, the voltage lower than the dielectric breakdown voltage of the electrode gap. The discharge is then initiated by charged particles contained in the vapour cloud entering the gap. The cross discharge should only be effective during the residence time of the laser-produced vapour in the gap. It has been shown that a free choice of the onset of the discharge may give better analytical results than automatic triggering. The cross discharge source closely resembles a customary spectrochemical medium voltage spark source. Therefore, the resulting spectra are also very similar with the result that the spectral lines are much narrower and the spectral background lower as compared to those in the primary spectrum of the laser-produced vapour plume. The intensity ratio of line-to-background is improved



by orders of magnitude in favourable cases, and consequently, the power of detection. The gross intensity of the emerging radiation may also be higher by up to two orders of magnitude. As a disadvantage it may be stated that impurities in the auxiliary electrodes cannot be distinguished by their signals from those in the analytical sample. To overcome this ambiguity, electrodeless discharges have been recommended.

The vapour can either be produced directly in the excitation zone of an induction coupled plasma (ICP) or a microwave induced plasma (MIP) or it can be transferred into it with the help of a carrier gas. All these methods are treated in detail in <sup>3,4,5</sup>. Some recent results shall be briefly mentioned.

Dimitrov et al. <sup>8</sup> investigated the influence of gas mixtures on the limit of detection with spark cross excitation. They obtained the best results when using pure Argon. In another paper, Dimitrov and Maximova <sup>9</sup> improved the power of detection by inclining the sample surface in respect to the direction of the laser radiation, probably causing a decrease of absorption of the laser radiation in the vapour cloud. Nickel et al. <sup>53,54</sup>, in an extensive study, optimized conditions for quantitative local analysis of graphite with emphasis on good time matching of evaporation and cross excitation. Uchida et al. <sup>32</sup> concentrated element traces on filter paper after solvent extraction and subjected them to laser vaporization with cross excitation in a spark discharge. Leis and Laqua <sup>50,51</sup> used additional excitation in an MIP, the sample being directly part of the microwave cavity. Limits of detection in the  $\mu\text{g/g}$  range were obtained. Ishizuka and Uwamino <sup>42</sup> introduced a laser-produced aerosol into a MIP, obtaining limits of detection ranging from

1  $\mu\text{g/g}$  Zn in Al to 22  $\mu\text{g/g}$  Mn in steel with relative standard deviations from 0.01 to 0.13. Bachurina et al. <sup>22</sup> transferred the laser-produced aerosol to a CMP (capacitively coupled microwave plasma) for the determination of the alkaline and earth alkaline elements and iron in surface impurities of silicon sheets in the nanogram range. Thompson et al. <sup>56,57</sup> used the combination of laser and ICP and compared the results with standard ICP analysis of the dissolved steel samples. Generally, with laser, absolute detection limits were lower as compared to the nebulization technique, whereas with concentrational limits of detection it was the other way round.

#### 7. Laser Atomizers in Mass Spectrometry

The ions formed in the vapour cloud as a result of the action of focused laser radiation on a solid surface can be separated and detected with a mass spectrometer. In this way, combination of a laser with a mass spectrometer permits the construction of instruments for bulk as well as local or microprobe analysis. Both, double-focusing and time-of-flight mass spectrometers have been used. Earlier work has been fully covered by Conzemius and Capellen <sup>62</sup> in their review article. The modern state of the art regarding bulk analysis, microanalysis and thin film analysis of moderate spatial resolution (crater diameters about 20  $\mu\text{m}$ , crater depths ranging from 0.1 to 10  $\mu\text{m}$ ) is represented by the work of Jansen and Witmer <sup>63,64</sup>. They used a Q-switched Nd:YAG laser system as an ion source, Fig. 7, and an AEI MS 702 double-focusing mass spectrometer with photographic detection. This permits detection of ions in the mass range between 6 and 240 AMU with good resolution, irrespective of the considerable energy spread of the laser-produced ions.

An absolute detection limit of about  $10^{-12}$  g, a relative detection limit of 10 ng/g for bulk, and 1 mg/g for micro-analysis can be obtained. The precision can be described by a relative standard deviation of about 0.2, the accuracy by a factor of 2 without and 0.2 with standards.

A completely different line of development has been pursued by Hillenkamp et al.<sup>66</sup> resulting in a laser microprobe mass analyzer (LAMMA) of which a commercial model, the LAMMA-500, (Leybold-Heraeus) is available. Fig. 7 shows the principles of this instrument, in which a Nd:YAG laser irradiates the sample which may be a foil or a thin layer on a transparent substrate. The ions formed enter a time-of-flight mass spectrometer for separation and detection by an open Cu-Be secondary electron multiplier. The system is preferentially used for the analysis of thin samples, mostly biological material. Absolute detection limits lie in the range of  $10^{-18}$  to  $10^{-20}$  g. Under favourable circumstances (very thin films) a lateral resolution of less than 1  $\mu$ m is obtainable. Not only atoms, but molecules as well can be detected.

A similar instrument has been described by Dingle and Griffith<sup>71</sup> which in addition, enables the analysis of bulk samples by means of reflected ions. A compensation for the initial spread of energy of the ions is also provided.

## 8. Laser Spectrochemical Procedures

8.1 Local analysis. A microanalysis performed in situ may be called local analysis. Typical examples are an inclusion in a metal or mineral or the changing composition along a welding seam. In such cases, spatial resolution and the con-

centration range of the elements to be determined influence significantly the choice of laser operating parameters, spectral apparatus and radiation detector. For a one-shot analysis with no additional excitation, Q-switched lasers producing craters of about 50  $\mu$ m diameter may yield line intensities which are sufficiently strong to be recorded with a high speed spectrograph (f/5 or better) if only the main constituents of a sample have to be determined. With additional excitation and free running lasers, usable analytical signals can be obtained from craters with a diameter of about 10  $\mu$ m. In this case, a medium speed spectrograph may be sufficient. Photoelectric detection is much more sensitive but does not easily permit the recording of a substantial part of the spectrum. An interesting attempt has been made by Talmiet al.<sup>39</sup> to overcome these difficulties. They used SIT-vidicons and second generation photodiode arrays as detectors and obtained limits of detection between 2 and 500  $\mu$ g/g in surface analysis and depth profiling. Unfortunately, present day vidicons and silicon photodiode arrays cannot optimally be matched to commercial spectral apparatus. In Table 2 the properties of laser local analysis are summarized.

8.2 Surface Analysis and Depth Profiling. Surface analysis represents local analysis in which the depth of erosion is kept as small as possible. Either a free running laser of very low output energy and additional excitation or a Q-switched low-energy, high-power giant pulse should be used. The former may yield crater diameters of 10  $\mu$ m with a depth of 3  $\mu$ m, the latter diameters of about 25  $\mu$ m and a depth of 1  $\mu$ m depending also on the sample material.

8.3 Microanalysis. Techniques for microanalysis are similar to those for local analysis. A microsample must be transformed into a small volume and then atomized for local analysis. For minimum matrix effects, the sample should be vaporized completely. The amount of sample can be as low as 1 µg. Limits of detection down to 10 µg/g can be achieved, depending on the element and the size of the sample.

8.4 Macro- or Bulk Analysis. Because of the unique property of laser atomization, homogeneous, non-conducting solid materials in addition to electrically conducting materials can be directly analysed by means of optical spectroscopy. There is some reason to recommend laser atomization for electrically conducting materials normally analysed with the help of spark discharges. In electrical discharges, the burning spot wanders erratically across the surface which may give rise to systematic errors if that movement is influenced by a structure of the surface. Attempts have therefore been undertaken to prevent the wandering of the burning spot by means of focused laser radiation<sup>19</sup> resulting in improved precision and accuracy.

In laser analysis of homogeneous samples, precision can be improved by increasing the number of shots per analysis. This should be done by automatic scanning of the surface in such a way that by each laser shot, a hitherto unattacked part of the surface is sampled. The basic obtainable precision depends on the mode of operation. It can be as good as 0.1 for a single shot without additional excitation and correspondingly less for a multishot analysis. If high power of detection is required and hence, additional excitation, the basic precision may

degrade to about 0.3. These figures apply to laser output energies of about 1 joule which corresponds to vaporized sample material of about 10 µg per shot. Sampling of much more material for a single-shot analysis with laser output energies of up to 100 joule has been reported. A good compromise would be a multishot analysis with energies of about 5 joule per shot. In macro-analysis, non-compromise conditions can be selected for good power of detection. In Table 3, some typical examples are given.

8.5 Special Procedures. Artificial gas atmospheres and pressures other than ambient can be used to further optimize analytical conditions. As already mentioned and confirmed by other investigators, argon seems to be favourable for high intensity of the spectral lines and reduced background. For the best line-to-background ratio vacuum was established as optimum.

The laser cloud is inhomogeneous and very transient in time and space. By time-resolving and gating of the analytical signal conditions for optimum line-to-background ratio can be established. Space-resolved spectroscopy can be successfully applied whenever the analysis is performed without auxiliary excitation due to the fact that spectral lines and spectral background have their maximum intensity in different zones of the laser plume. Finally, a magnetic field may also be used to improve line-to-background ratios and consequently, the power of detection. The best results in taking account of many single step improvements have been reported by Treytl et al.<sup>73</sup> Table 5 lists some of their results. It should further be noted that this group, in favourable cases, was able to

secure from biological materials, useful analytical signals from craters of about 1  $\mu\text{m}$  diameter.

In an interesting application, Adrian et al.<sup>29</sup> used a computerized laser-micro-spectrograph equipped with a SIT-vidicon for remote analysis at a nuclear reactor. Radiation from the laser head with additional excitation was conducted to the spectral apparatus by means of an optic fibre of 40 mm length.

#### 9. Conclusion

Atomization by means of focused laser radiation has supplemented the analytical repertoire considerably due to its applicability to all kinds of samples, irrespective of their chemical and physical conditions. Originally introduced for local and microanalysis by optical emission spectroscopy, it is now also used for bulk and surface analysis of a large variety of materials, in combination with other spectroscopic methods like AAS and mass spectrometry. Whereas up to now, mostly qualitative and semiquantitative procedures have been described, there are high precision procedures available waiting for their introduction into analytical practice. Reliable calibration in local analysis remains a problem which needs further attention. Laser sources for atomization have been developed to a high degree of perfection and can be operated reliably and at low costs. Excimer lasers may find special uses resulting from their high power output and high repetition rates.

#### References

1. T.H. Maiman, 'Stimulated Optical Radiation in Ruby', *Nature*, 187: 493 (1960).
2. F. Brech and L. Cross, 'Optical Microemission Stimulated by a Ruby MASER', *Appl. Spectrosc.*, 16: 59 (1962).
3. R.H. Scott and A. Strasheim, 'Laser Emission Excitation and Spectroscopy',  
*in: Applied Atomic Spectroscopy*, Vol. 1, by E.L. Grove, ed., Plenum Press, New York and London, 1978.
4. K. Laqua, 'Analytical Spectroscopy using Laser Atomizers',  
*in: Analytical Laser Spectroscopy* by N. Omenetto, ed., John Wiley & Sons, New York, Chichester, Brisbane, Toronto, 1979.
5. M.L. Petukh and A.A. Yankowskii, 'Atomic Emission Spectral Analysis using Lasers', *Zh. Prikl. Spektrosk.*, 29:1109 (1978).
6. H. Moenke and L. Moenke-Blankenburg, 'Laser Micro-Spectrochemical Analysis', Adam Hilger, London, 1973.
7. W. van Deijck, J. Balke and F.J.M.J. Maessen, 'An Assessment of the Laser Microprobe Analyser as a Tool for Quantitative Analysis in AES', *Spectrochim. Acta*, 35 B: 359 (1979).
8. G. Dimitrov, L. Nikolova and Ya. Vasilev, 'Influence of the Discharge Gas on the Emission and Thermal Characteristics of Laser-induced Microplasmas', *Mikrochim. Acta*, 1: 503 (1979).
9. G. Dimitrov, Ts. Maximova, 'Improvement of the Reproducibility and Sensitivity of Laser Microspectral Analysis', *Spectroscopy Letters*, 14: 737 (1981).
10. E.K. Vul'fson, V.I. Dvorkin and A.V. Karyakin, 'The Problem of Vaporization of a Substance in a Laser Jet', *Zh. Prikl. Spektrosk.*, 32: 414 (1980).

11. V.A. Ageev, A.V. Kolesnik and A.A. Yankovskii, 'Laser Determination of Electroplating Thickness', Zh. Prikl. Spektrosk., 26: 360 (1977).
12. A.F. Bokhonov, V.S. Burakov, V.V. Zhukovskii and A.A. Stavrov, 'Erosion Due to Radiation Activity of Lasers in the Mode-Locked Regime', Zh. Prikl. Spektrosk., 26: 821 (1977).
13. S.I. Anisimov, Ya. A. Imas, G.S. Romanov, Yu.V. Khodyko, 'The Effect of High Power Radiation on Metals' (in Russian), Nauka, Moscow (1970)
14. M.F. Stel'makh, 'Lasers in Technology', (in Russian), Energiya, Moscow, (1975).
15. S.P. Atamanova, 'LMA-1 Apparatus for the Microspectral Analysis of Certain Minerals found in the Kolsk Peninsula', Zh. Prikl. Spektrosk., 32: 202 (1980).
16. M.L. Petukh, A.D. Shirokanov and A.A. Yankovskii, 'Use of Laser Pulses with Electric Discharges for Atomic Absorption Analysis', Zh. Prikl. Spektrosk., 32: 414 (1980).
17. A.A. Yankovskii, 'Quantum Electronics and Laser Spectroscopy' (in Russian) Nauka i Tekhnika, Minsk (1979) Chap. XVIII, p. 362
18. A.N. Zaidel, G.V. Ostrovskaya and Yu.I. Ostrovskii, 'Technique and Application of Spectroscopy' (in Russian), Nauka, Moscow (1972).
19. V.A. Ageev, A.V. Kolesnik and A.A. Yankovskii, 'Possibility of Limiting the Migration of Current-Carrying Discharge Channels by a Laser Beam', Zh. Prikl. Spektrosk., 26: 417 (1977).
20. W. Maul and W. Quillfeldt, 'Homogeneity Investigation with the LMA 10 Laser Microspectral Analyser', Jena Review, 22:234 (1977).
21. E.Litz, 'Staubanalysen mit dem Laser-Mikrospektral-Analysator LMA 10', Jenaer Rundschau, 5:237 (1977).
22. L.G. Bachurina, V.M. Perminova and S.A. Savostin, 'Spectral Micro-Analysis with Laser and Plasma Excitation of the Spectra', Zavodsk. Lab. 45: 1113 (1979).
23. D.E. Maksimov, N.K. Rudnevskii, V.P. Ryabchikova and E.N. Pryanichnikova, 'Laser Spectral Micro-Analysis of Welded Seams', Zavodsk. Lab., 45: 333 (1979).
24. D.E. Maksimov, N.K. Rudnevskii, V.P. Ryabchikova, S.M. Chekhonin, I.V. Shlyapnikov and I.S. Shklyayeva, 'LMA-1 Laser Microanalyzer Applied to Welds in Alloy Steels', Zavodsk. Lab., 43: 445 (1977).
25. M.B. Kozik, 'Modification of a Quantitative Laser-Spectrographic Method of Determination of Cations Contained in Tissue Slices', Folia Histochem. Cytochem., 17:153 (1979).
26. W. Klimecki, 'Local Spectral Analysis and Lasers', Chem. Anal. (Warsaw), 23: 3 (1978).
27. R.M. Manabe, 'Effects of Atmospheric Pressure on Line Widths and Spatial Distributions of Transient AA Signals of Minor Constituents in Metal Samples Atomized by a Dye Laser Microprobe', Dissertation, Oregon, State University (1977).
28. M.B. Kozik, 'Laser-spectrographic Study on the Contents of Metals in Brains of Patients with Arteriosclerotic Dementia', Folia Histochem. Cytochem., 16: 31 (1978).
29. R.S. Adrain, R.C. Klewe and E.J. Ormerod, 'Robust Portable Computerised Laser Micro-spectrograph',  
in: Conf. Proceed. 'Electro-Optics Laser International '80, ICP Science and Technology Press, Ltd.
30. R.S. Adrain, D.R. Airey, R.C. Klewe and E.J. Ormerod, 'Trace Element Line Intensities in Laser produced Metal Vapour Plasmas', Private communications.

31. R.S. Adrain, J. Watson, P.H. Richards and A. Maitland,  
'Laser Microspectral Analysis of Steels', Optics and  
Laser Technology, 12: 137 (1980).
32. H. Uchida, K. Iwasaki, 'Laser-microprobe Spectroscopy for  
Trace Elements Concentrated on Filter-paper after Solvent  
Extraction', Bunseki Kagaku, 25: 752 (1976).
33. T. Ishizuka, Y. Uwamino and H. Sunahara, 'Laser-Vaporized  
Atomic Absorption Spectrometry of Solid Samples',  
Anal. Chem., 49: 1339 (1977).
34. J. Kozak, 'Correction for the Volume of Vaporized Material  
in Laser Spectral Analysis', Chem. Listy., 71: 424 (1977).
35. M. Hufner, 'Using the KSR 4200 small Process-control Compu-  
ter with Laser Emission Spectrochemical Analysis'  
Jena Review, 21: 312 (1976).
36. J.M. Green, W.T. Silfvast and O.R. Wood, 'Evolution of a  
Co<sub>2</sub>-Laser-produced Cadmium Plasma', J.Appl.Phys., 48:2753  
(1977).
37. G. Dimitrov and I. Koleva, 'Investigations of Sparking with  
the Aid of a LMA-1 Laser Microspectral Analyser',  
Chem. Anal. (Warsaw), 22: 861 (1977).
38. E. Raitieri, M. Guerzoni and G. Grammatica, 'Use of Micro-  
probe Laser in Emission Spectrography', Met.Ital., 73:173  
(1981).
39. Y. Talmi, H.P. Sieper and L. Moenke-Blankenburg, 'Laser-  
Microprobe Elemental Determinations with an Optical Multi-  
channel Detection System', Anal. Chim. Acta, 127 : 71 (1981).
40. A.V. Karyakin, E.K. Vul'fson and A.F. Yanushkevich,  
'Über die Möglichkeiten und Grenzen der Anwendung des Laser-  
Atomisators für die Analyse fester Proben', Publ. Technische  
Hochschule Karl-Marx-Stadt (1976).
41. J. Mohr, 'Probenkammer mit Versorgungseinheit zum Laser-  
mikrospektral-Analysator LMA 10', Jenaer Rundschau,  
24 : 245 (1979).
42. T. Ishizuka and Y. Uwamino, 'Atomic Emission Spectrometry  
of Solid Samples with Laser Vaporization - Microwave-Induced  
Plasma System', Anal. Chem., 52: 125 (1980).
43. K. Sumino, R. Yamamoto, F. Hatayama, S. Kitamura and H. Itoh,  
'Laser Atomic Absorption Spectrometry for Histochemistry',  
Anal.Chem., 52 : 1064 (1980).
44. K. Dittrich and R. Wennrich, 'AAS using Laser-vaporization  
followed by ETA', Spectrochim.Acta, 35B: 731 (1980).
45. E.K. Wulfson, W.I. Dworkin and A.W. Karyakin, 'Measurements  
on the Thermal Conditions in the Vapour Cloud Produced by  
Laser Impact on Graphite', Spectrochim.Acta, 35B : 11 (1980).
46. R.M. Manabe and E.H. Piepmeier, 'Time and Spatially Resolved  
Atomic Absorption Measurements with a Dye-Laser Plume  
Atomizer and Pulsed Hollow-cathode Lamps', Anal. Chem.,  
51 : 2066 (1979).
47. W. Quillfeldt, 'Combination of AAS and AES with the Laser  
spectrometer LMA 10', Jena Review, 23 : 226 (1978).
48. A. Quentmeier, K. Laqua and W.-D. Hagenah, 'Atomic-Absorption  
Spectrometry by Laser-Radiation Evaporation of Solid Samples.  
I. Optimization of Experimental Parameters,'  
Spectrochim. Acta 34 B : 117 (1979).
49. A. Quentmeier, K. Laqua and W.-D. Hagenah, '  
Atomic Absorption Spectroscopy of Solid Samples using Eva-  
poration by Laser Radiation. II. Analytical Applications,'  
35 B : 139 (1980).

50. F. Leis and K. Laqua, 'Emission Spectrometric Analysis using Microwave Excitation of a Vapour Cloud Produced by Laser Impact on a Solid. 1. Principles of the Method and Experimental Realization', *Spectrochim. Acta*, 33B : 727 (1978).
51. F. Leis and K. Laqua, 'Emission Spectrometric Analysis using Microwave Excitation of a Vapour Cloud Produced by Laser Impact on a Solid. II. Analytical Applications', *Spectrochim. Acta* 34 B : 307 (1979).
52. R.M. Measures and H.S. Kwong, 'TABLASER: Trace (element) Analyser based on Laser Ablation and Selectively Excited Radiation', *Appl. Opt.*, 18 : 281 (1979).
53. H. Nickel, F.A. Peuser and M. Mazurkiewicz, 'Evaporation of Material and Influence of Auxiliary Spark Gap on the Spectral Excitation by Means of Laser Emission Spectroscopy for Local Analysis of Graphite', *Spectrochim. Acta*, 33B : 675 (1978).
54. H. Nickel, F.A. Peuser, M. Mazurkiewicz and W. Dörge, 'Quantitative Mikroanalyse von Reaktorgrafit mit Hilfe der Laser-Emissions-Spektroskopie', *Jenaer Rundschau*, 5:199 (1979).
55. S.O. Baisane, V.S. Chincholkar and B.N. Maltor, 'Laser-Mikrospektralanalyse - Einige forensische Applikationen' *Jenaer Rundschau*, 5 : 206 (1979).
56. M. Thompson, J.G. Goulter and F. Sieper, 'Verdampfung fester Proben im Laserstrahl des LMA 10 und ihre Zuführung in induktiv-gekoppeltes Plasma (ICP) für die Atom-Emissionsspektrometrie', *Jenaer Rundschau*, 5 : 202 (1981).
57. M. Thompson, J.G. Goulter and F. Sieper, 'Laser Ablation for the Introduction of Solid Samples into an Inductively Coupled Plasma for Atomic-emission Spectrometry', *Analyst*, 106 : 32 (1981).
58. R.M. Measures and H.S. Kwong, 'Trace Element Laser Micro-analyser with Freedom from Chemical Matrix Effect', *Anal. Chem.*, 51 : 428 (1979).
59. D.C. Smith, 'Laser Radiation-induced Air Breakdown and Plasma Shielding', *Opt. Engineering*, 20: 962 (1981).
60. Kh.I. Zil'bershtein, 'Modern Light Sources for Analysis of Optical Emission Spectra', *Zavodsk. Lab.*, 46:1095 (1980).
61. R.E. Honig and J.R. Woolston, 'Laser-induced Emission of Electrons, Ions and Neutral Atoms from Solid Surfaces', *Appl. Phys. Lett.*, 2 : 138 (1963).
62. R.J. Conzemius and J.M. Capellen, 'A Review of the Application to Solids of the Laser Ion Source in Mass Spectrometry', *Int. J. Mass Spectrom. Ion Phys.*, 34:197 (1980).
63. J.A.J. Jansen and A.W. Witmer, 'Spark Source Mass-Spectrometry in the Research Laboratories of an Electronic Industry' *Fresenius Z. Anal. Chem.* 309 : 262 (1981).
64. J.A.J. Jansen and A.W. Witmer, 'Quantitative Inorganic Analysis by Q-switched Laser Mass Spectroscopy', *Spectrochim. Acta*, 37B : 483 (1982).
65. E. Denoyer, R. van Grieken, F. Adams and D.F.S. Natusch, 'Laser Microprobe Mass Spectrometry- I. Basic Principles and Performance Characteristics', *Anal. Chem.* 54:26 A (1982).
66. F. Hillenkamp, E. Unsöld, R. Kauffmann and R. Nitsche 'Laser microprobe Mass Analysis of Organic Materials' *Nature*, 256 : 119 (1975).
67. M.H.R. Hutchinson, 'Excimer and Excimer Lasers', *Appl. Phys.*, 21 : 15 (1980).

Table 1 Some Properties of Lasers suitable for Atomization of Solid Samples

Type of laser	Wavelength $\lambda$ $\mu\text{m}$	Excitation	Output energy of free-running laser, J	Range of power per pulse, MW	Angle of divergence mrad	Repetition rate pps
Solid state						
Ruby	0.6943* }	optically	10	0.1-10	3-5	low
Mt-glass	1.06 * }	pumped	10	0.01-10	5	low
Mt: YAG	1.06 * }		10	0.01-0.1	3-5	$10^3$
Fluid state						
Mt: $\text{POCl}_3$	1.06 }	optically	5	~10	~10	10
Mt: $\text{SeOCl}_2$	1.06 }	pumped	1	~0.1	2	100
Gaseous state						
$\text{CO}_2$ -TEA	10.6 }	electrically	100	~1	5	100
$\text{N}_2$	0.337 }	excited	0.01	~0.1	~10	100
Excimer	0.193-0.351	electrically	~0.2	~20	2x4	100
Oscillator		excited				
Excimer	0.193-0.351	electrically	~0.3	~15	0.2	40
Oscillator		excited				
+ Amplifier						

\* also used at  $\lambda/2$ ,  $\lambda/3$  and  $\lambda/4$  obtained by frequency multiplication.

68. P. Boissel, G. Bauchecorne, P. Morleve and G. Mayer,

'Optical Elements using Oscillating Gases',  
Opt. Communications, 4 : 44 (1971).

69. J.F. Ready, 'Effects of High-Power Laser Radiation'  
Academic Press, New York and London, 1971.

70. T.C. Moseotti, K. Laqua and W.-D. Haggenb, 'Laser-Micro-  
analysis by Atomic Absorption', Spectrochim.Acta,  
B2B : 157 (1967).

71. J. Dingle and B. Griffith, 'A Laser Ion Mass Analyser  
(LIMA) for Bulk Samples with High Spatial Resolution and  
PPM Hydrogen Sensitivity', J.Phys.E,Scient.Instrum. 14 : 513 (1981)

72. U. Mde, 'Extension and Enhancement of the Spectral Emission  
of Radiation from Samples Micro-sized by Laser Particles',  
J.Phys.E,Scient.Instrum. 14 : 513 (1981)

73. J.L. Smith, J.L. Green, J.L. Smith, J.L. Smith and  
B. Hlick, 'Detection Limits in Analysis of Metals in  
Biological Materials by Laser Microprobe Optical Emission  
Spectroscopy', Anal. Chem. 50 : 1000 (1978).



Table 1 Some Properties of Lasers suitable for Atomization of Solid Samples

Type of laser	Wavelength $\lambda$ nm	Excitation	Output energy of free-running laser, J	Range of power per pulse, mW	Angle of divergence mrad	Repetition rate pps
Solid state						
Ruby	0.6943* }	optically pumped	10	0.1-10	3-5	low
Mt-glass	1.06 * }		10	0.01-10	5	low
Nd: YAG	1.06 * }		10	0.01- 0.1	3-5	10 <sup>3</sup>
Fluid state						
Nd: POC <sub>13</sub>	1.06 }	optically pumped	5	~10	~10	10
Nd: SeOCl <sub>2</sub>	1.06 }		1	~ 0.1	2	100
Dyes	0.22-0.74 }					
Gaseous state						
CO <sub>2</sub> -TEA	10.6 }	electrically excited	100	~ 1	5	100
N <sub>2</sub>	0.337 }		0.01	~ 0.1	~10	100
Excimer	0.193-0.351		~0.2	~20	2x4	100
Oscillator		excited				
Excimer	0.193-0.351	electrically	~0.3	~15	0.2	40
Oscillator + Amplifier		excited				

\* also used at  $\lambda/2$ ,  $\lambda/3$  and  $\lambda/4$  obtained by frequency multiplication.

Table 3

Limits of Detection ( $\mu\text{g/g}$ ) for some Elements in Optical Emission Spectrochemical Analysis pertaining to several Excitation Methods.

Analytical line, nm <sup>a</sup>	Laser source <sup>a</sup>	Crossexcitation <sup>a</sup>	85MHz ICP <sup>a</sup>	2,47GHz MIP <sup>b</sup>	Analytical line, nm <sup>b</sup>
Mg 285.2	10	0.9	0.2	0.4	Mg 279.6
"	20	6	4	2	"
"	-	1	-	-	"
"	-	6	3	2	"
"	20	1	1	-	"

<sup>a</sup> Values taken from Møde<sup>72</sup>

<sup>b</sup> Values taken from Leis et al<sup>51</sup>

Table 4

Use of Time Resolution for Obtaining Low Limits of Detection in Analytical Procedure for Analysis of Biologic Materials, Employing Q-switched Single Laser Pulse and Electronic Gating Technique<sup>a</sup>

Element	Wavelength, nm	Delay time, $\mu$ s	Integration time, $\mu$ s	Detection limit, pg
Li	610.4	4	5	0.2
Mg	279.6	4	7	0.002
Ca	393.4	5	15	0.01
Fe	302.0	10	6	0.3
Cu	324.8	15	3	0.002
Zn	213.9	5	2	0.05
Hg	253.7	7	3	0.3
Pb	405.8	16	5	0.1

<sup>a</sup> From Trexler et al.<sup>73</sup>

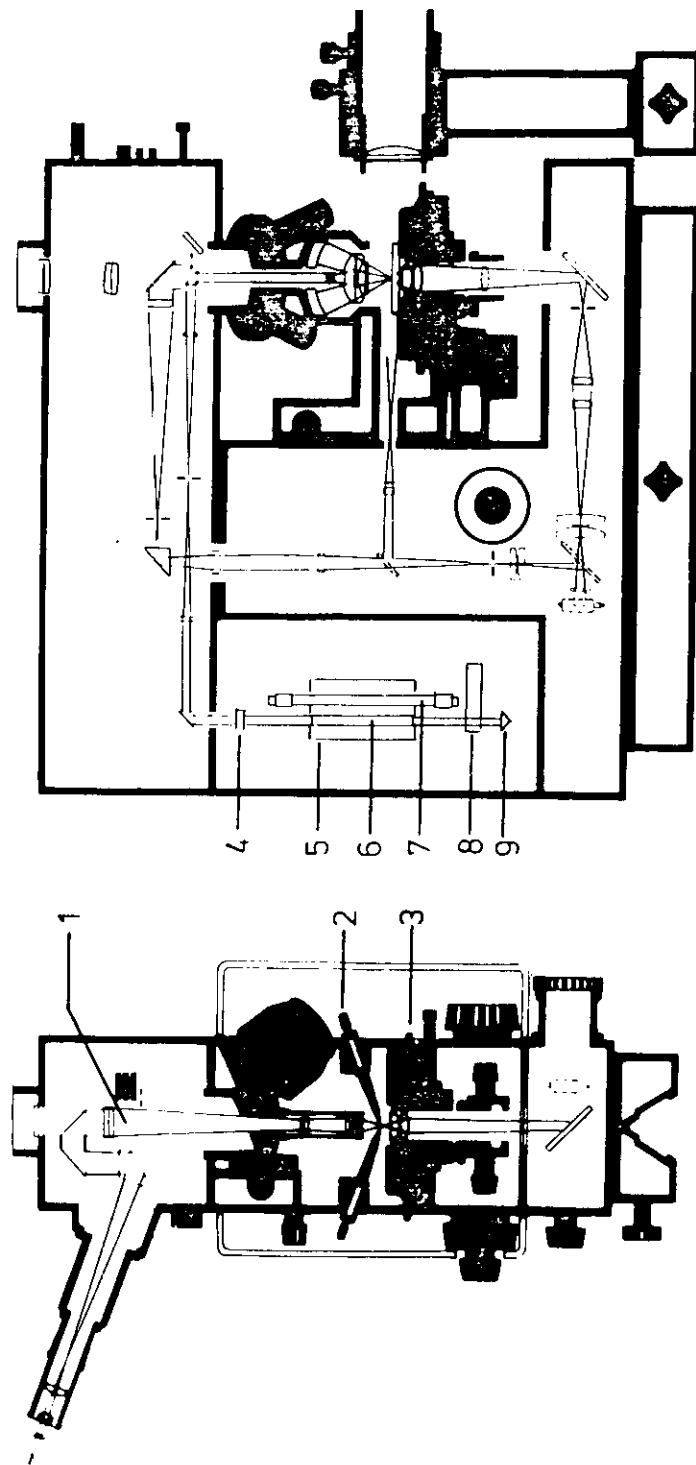


Figure 1: Laser Micro Analyticator LMA 10, Left, front view, right, side view, 1, observation microscope 2, electrodes for cross discharge, 3, microscope stage with sample holder, 4, semitransparent resonator mirror, 5, laser cavity, 6, laser rod, 7, flash-lamp for optical pumping, 8, liquid dye Q-switch, 9, resonator prism. VEB Carl Zeiss, Jena.

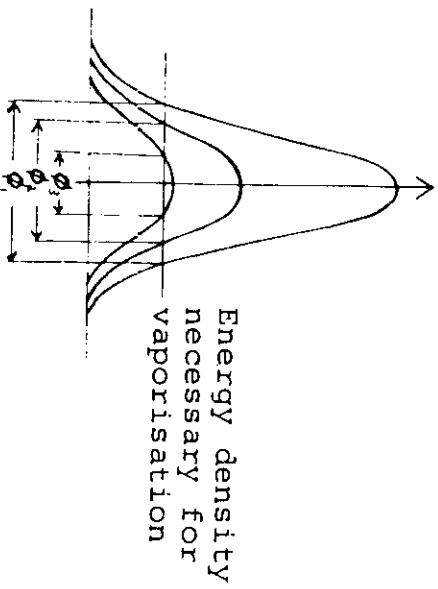
1. Focal length of the objective Focal area: $F = \pi \underline{f}^2 \tan^2 u$	Sample: Cu; Energy: 0,2 Joule <table><tr><td><math>\underline{f}</math></td><td><math>\underline{\phi}</math></td></tr><tr><td>8 mm</td><td>65 <math>\mu\text{m}</math></td></tr><tr><td>15 mm</td><td>81 <math>\mu\text{m}</math></td></tr></table>	$\underline{f}$	$\underline{\phi}$	8 mm	65 $\mu\text{m}$	15 mm	81 $\mu\text{m}$				
$\underline{f}$	$\underline{\phi}$										
8 mm	65 $\mu\text{m}$										
15 mm	81 $\mu\text{m}$										
2. Aperture of the laser beam $F = \pi \underline{f}^2 \tan^2 u$	Sample: Pb <table><tr><td></td><td><math>\underline{\phi}</math></td></tr><tr><td>with mode selection</td><td>114 <math>\mu\text{m}</math></td></tr><tr><td>without mode selection</td><td>342 <math>\mu\text{m}</math></td></tr></table>		$\underline{\phi}$	with mode selection	114 $\mu\text{m}$	without mode selection	342 $\mu\text{m}$				
	$\underline{\phi}$										
with mode selection	114 $\mu\text{m}$										
without mode selection	342 $\mu\text{m}$										
3. Energy of the laser pulse 	Sample: Co <table><tr><td>Energy</td><td><math>\underline{\phi}</math></td></tr><tr><td>1.40 Joule</td><td>80 <math>\mu\text{m}</math></td></tr><tr><td>0.48 Joule</td><td>64 <math>\mu\text{m}</math></td></tr><tr><td>0.24 Joule</td><td>48 <math>\mu\text{m}</math></td></tr><tr><td>0.13 Joule</td><td>25 <math>\mu\text{m}</math></td></tr></table>	Energy	$\underline{\phi}$	1.40 Joule	80 $\mu\text{m}$	0.48 Joule	64 $\mu\text{m}$	0.24 Joule	48 $\mu\text{m}$	0.13 Joule	25 $\mu\text{m}$
Energy	$\underline{\phi}$										
1.40 Joule	80 $\mu\text{m}$										
0.48 Joule	64 $\mu\text{m}$										
0.24 Joule	48 $\mu\text{m}$										
0.13 Joule	25 $\mu\text{m}$										

Figure 3 : Factors affecting diameter  $\phi$  of laser-produced crater, in a solid sample.

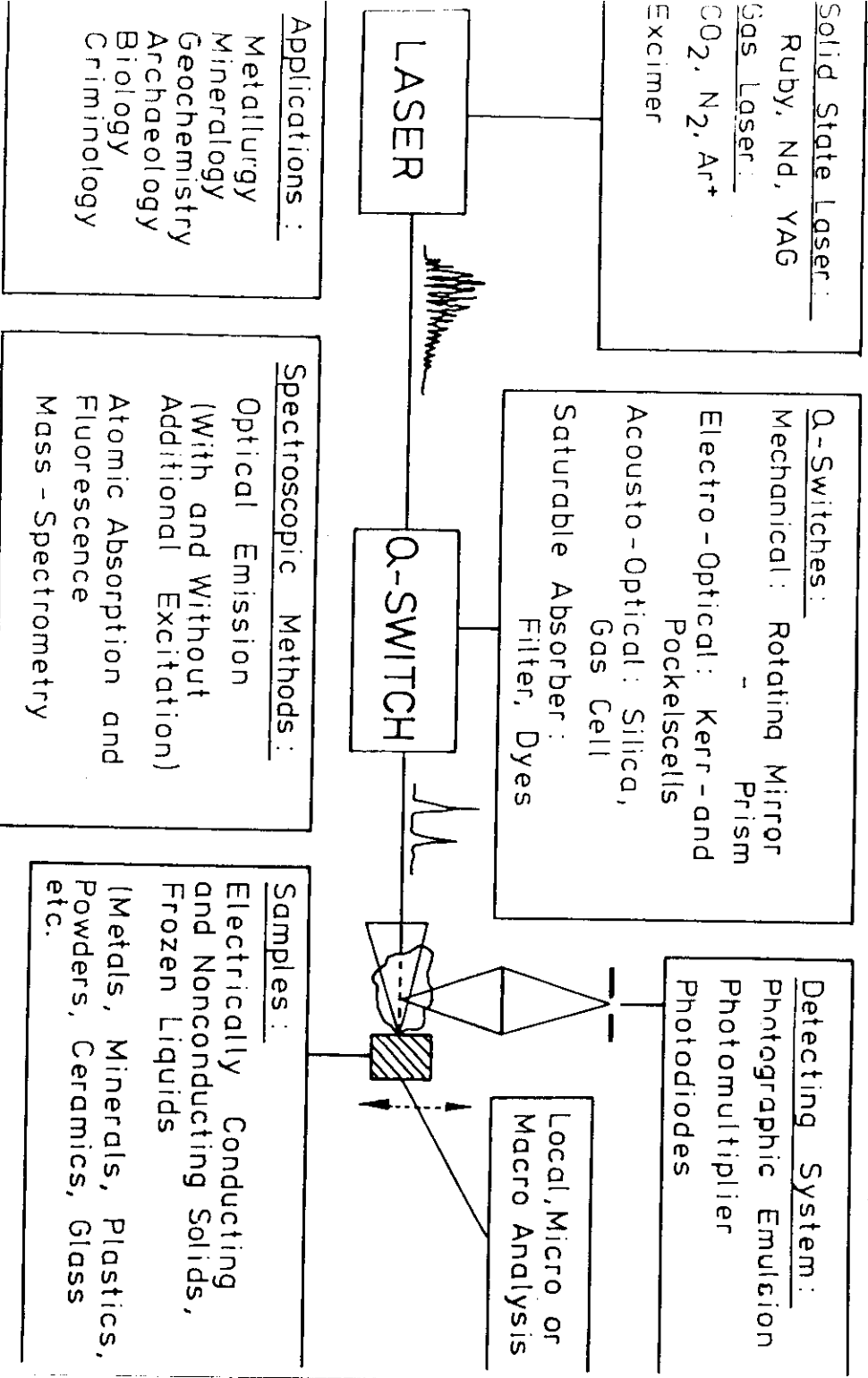
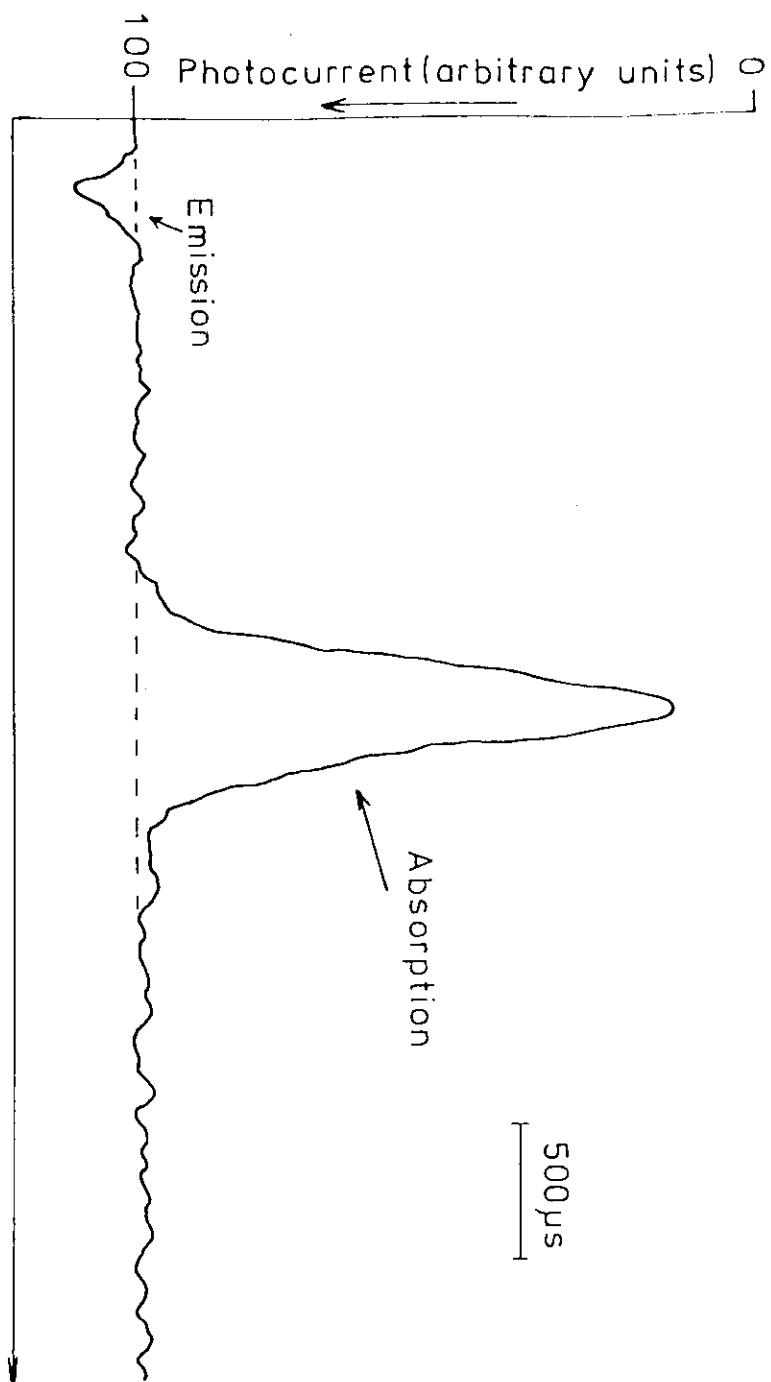
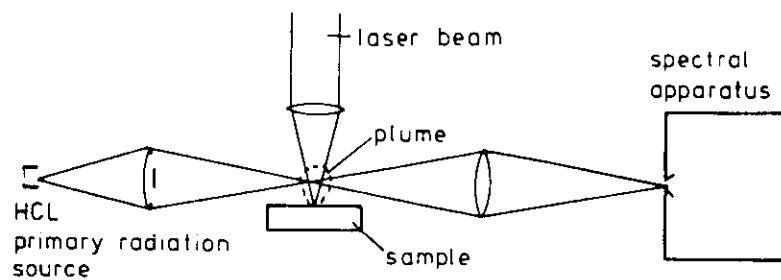


Figure 2 : Analytical possibilities in combination with laser atomizer.

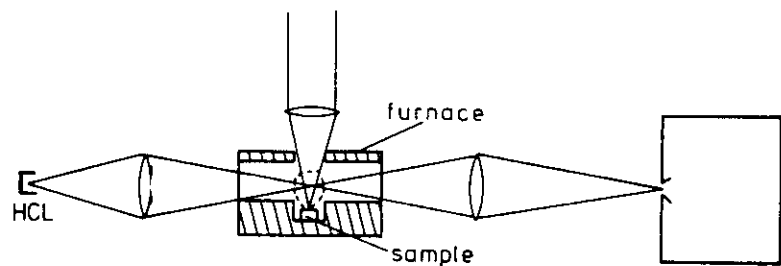
Figure 4 : Time dependence of the photocurrent during laser evaporation ( Height above sample surface, 25mm ).



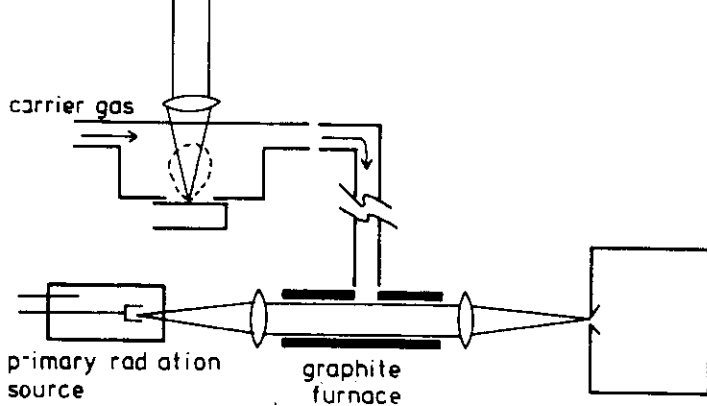
#### 1. Standard method



#### 2. Graphite furnace direct



#### 3. Graphite furnace transferred



#### 4. Flame

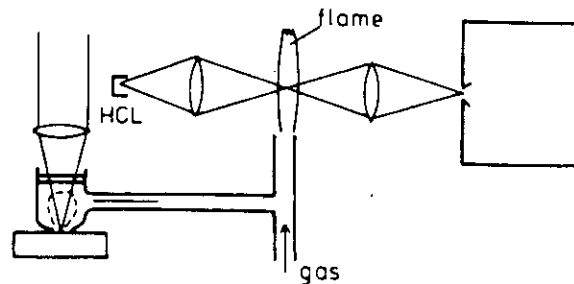


Figure 5 : Atomic absorption spectroscopy of laser vaporized

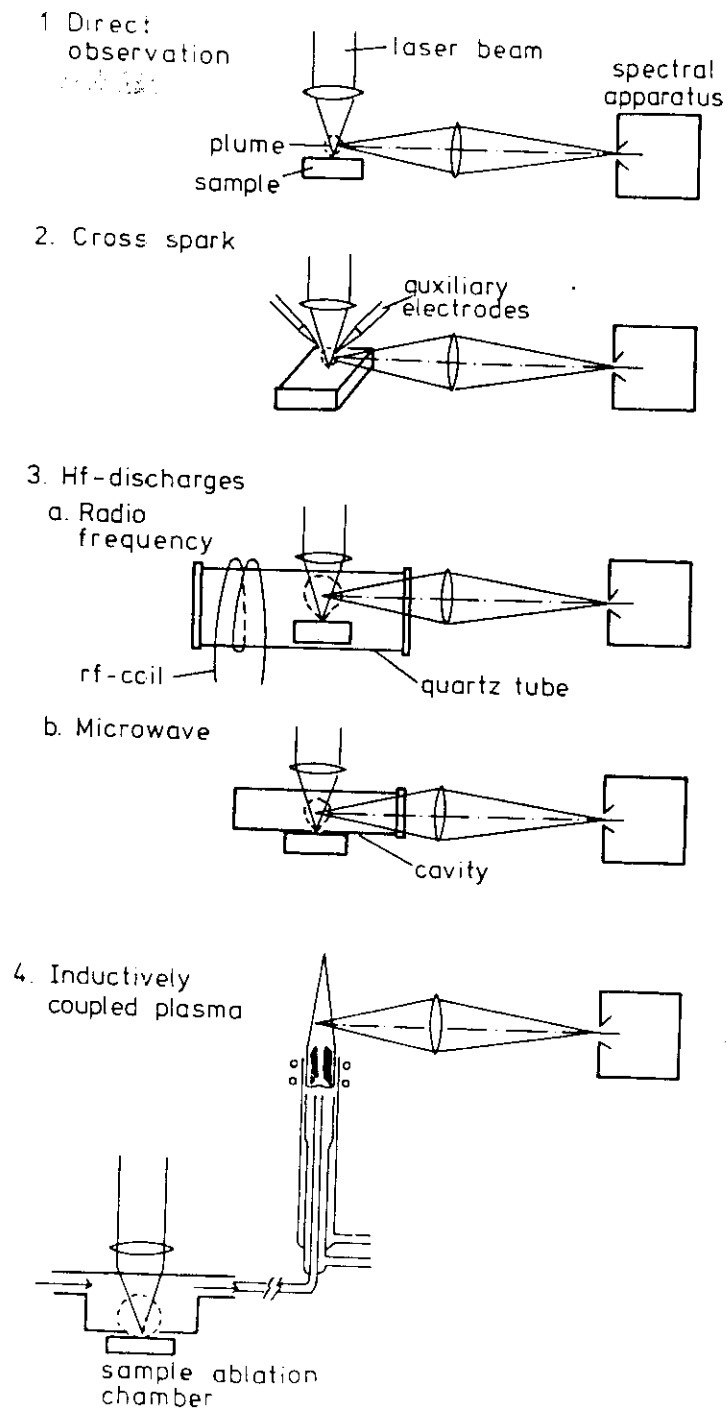


Figure 6 : Possibilities of optical emission spectroscopy with laser atomizers.

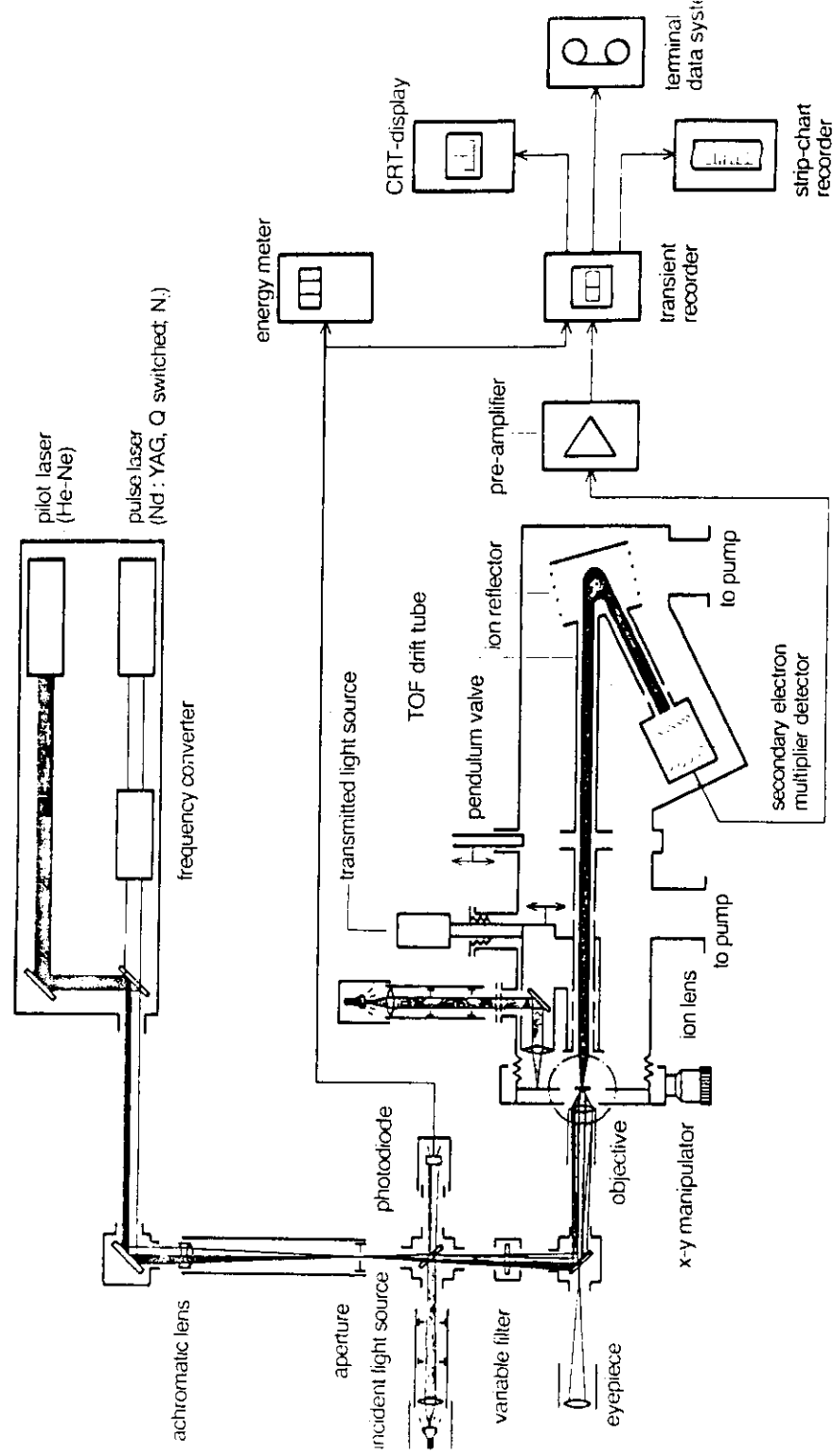


Figure 7 : Schematic diagram of LAMMA 500.

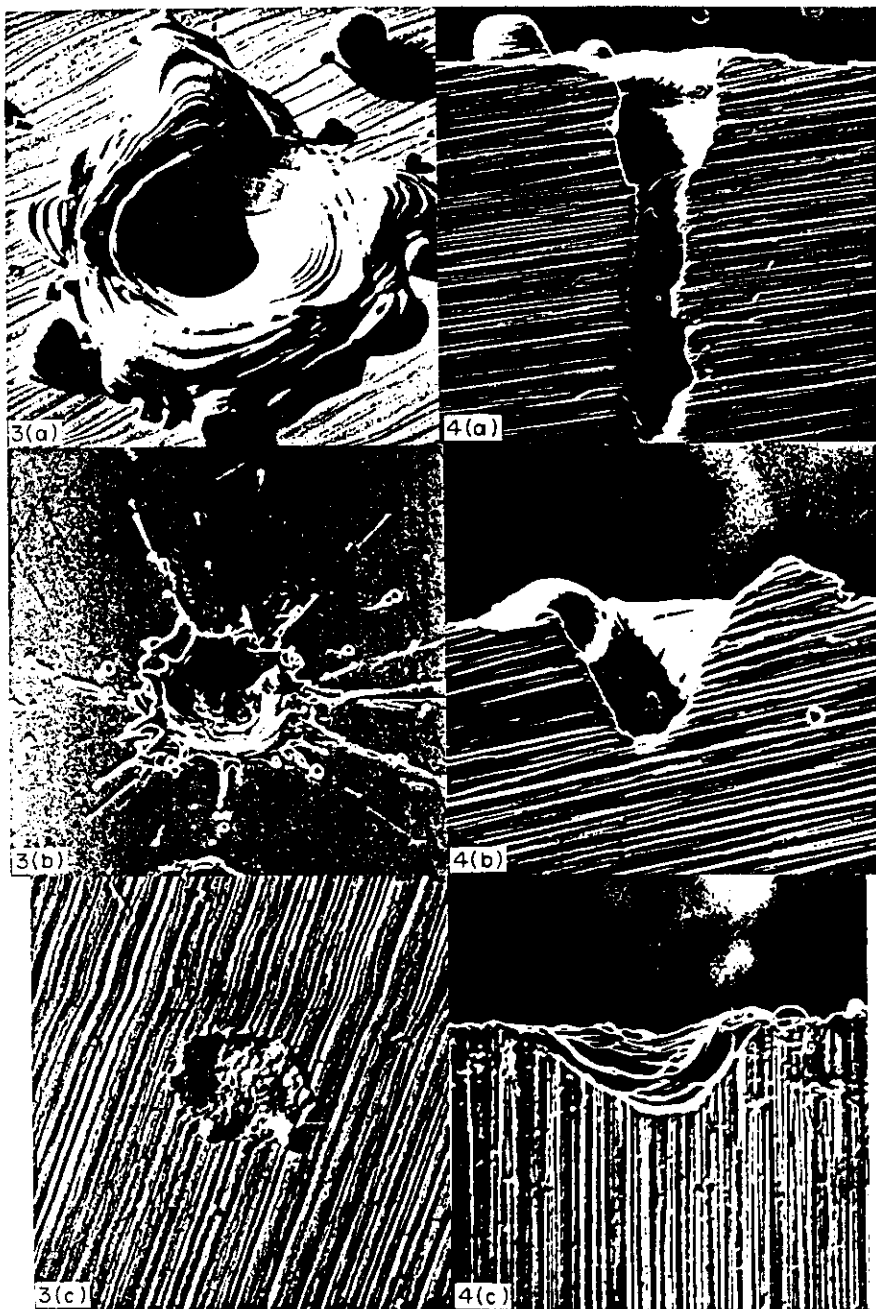


Abb. 3. (a)-(c) Verschiedene Laserkrater in Stahl, aufgenommen mit einem Rasterelektronenmikroskop Jeol JSM 35. Kantenlänge (a) 160  $\mu\text{m}$ , (b) 60  $\mu\text{m}$ , (c) 30  $\mu\text{m}$ .

Abb. 4. (a)-(c) Schliffbilder verschiedener Laserkrater in Stahl. Kantenlänge (a) 500  $\mu\text{m}$ , (b) 100  $\mu\text{m}$ , (c) 20  $\mu\text{m}$ .

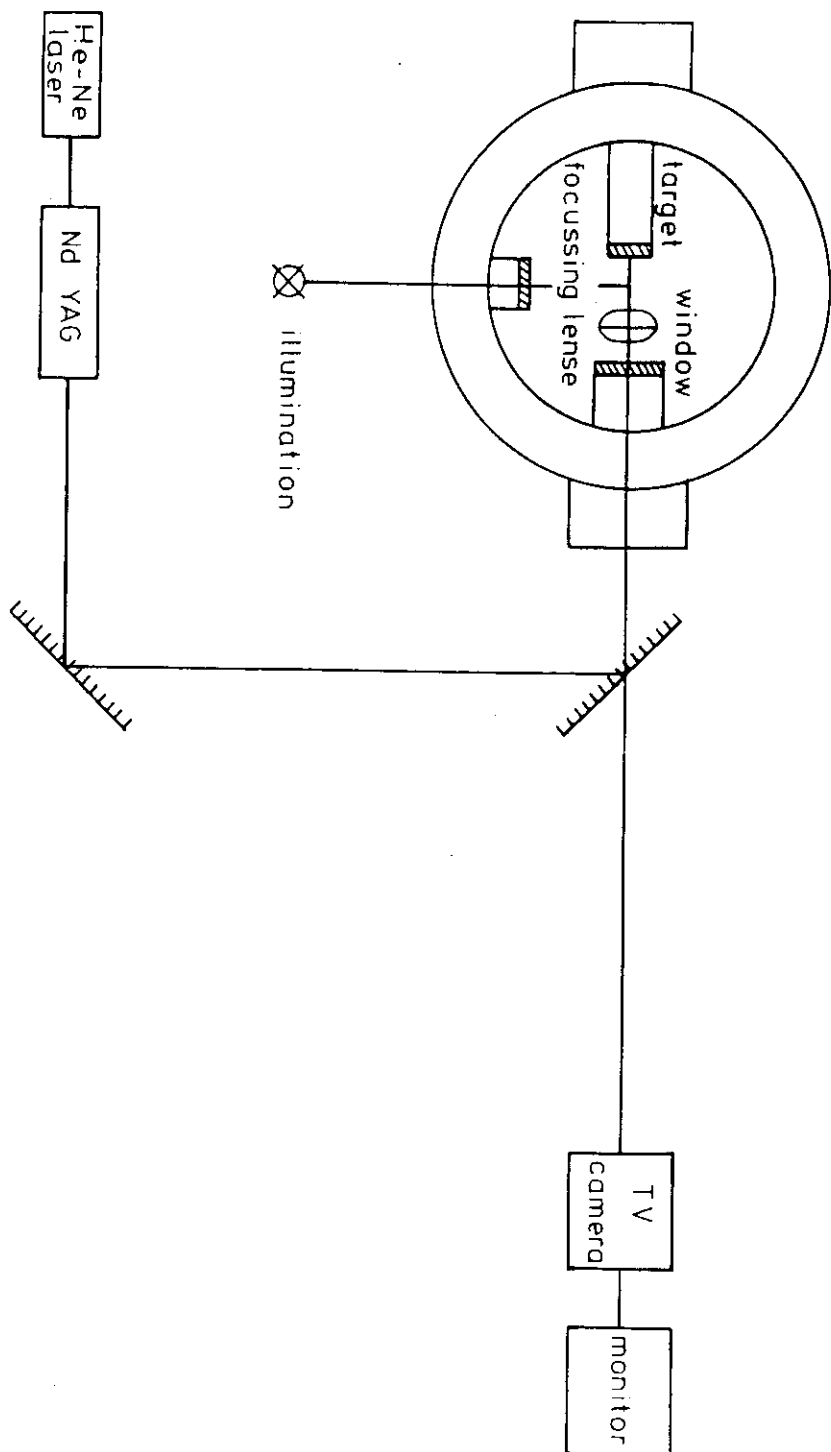


Figure 8 : Schematic structure of laser ion source system.

# Time-Resolved Laser-Induced Breakdown Spectrometry of Aerosols

Leon J. Radziemski,\* Thomas R. Loree, David A. Cremers, and Nelson M. Hoffman

University of California, Los Alamos National Laboratory, Chemistry Division, Los Alamos, New Mexico 87545

The repetitive breakdown spark from a focused laser beam was used to generate analytically useful emission spectra of aerosols in air. The apparatus is simple; a pulsed laser and optics, a spectrometer, and some method for time resolution of the spark light. Time resolution is essential because of the strong continuum emission at early times (<500 ns). High temperatures in the spark result in vaporization of small particles, dissociation of molecules, and excitation of atomic and ionic spectra. The plasma acts as if it were in local thermodynamic equilibrium, at least after 1  $\mu$ s. Spectroscopic methods have been used to measure the time-resolved temperatures and electron densities. A simple one-dimensional hydrodynamic model predicts the temperature and diameter of the spark. Beryllium in atmospheric pressure air has been detected at 0.7  $\mu$ g/m<sup>3</sup>, which is 0.6 ng/g of air (RSD = 30%). Limits of detection have also been established for Na, P, As, and Hg in air. A calibration curve linear over 4 orders of magnitude has been developed for Na in air. In situ experiments have been performed on two experimental coal gasification systems, and real-time spectral information has been obtained in both cases.

In atomic emission spectrochemistry, the light from an excited sample is spectrally analyzed to yield qualitative and quantitative information about the elemental constituents. The traditional emission techniques employ arc or spark excitation (1, 2) requiring electrodes. Recently atomic flame fluorescence (3) and the inductively coupled argon plasma (ICP) (4) have become accepted sources. None of the latter techniques are particularly useful for direct detection of aerosols in ambient air or usable outside of the analytical laboratory. The ICP (5) and the microwave-induced plasma (6) have been used to analyze vaporized material generated by a laser spark on a surface, by sweeping the material into the plasma with argon carrier gas. In this paper we discuss a field deployable variation of electrodeless spark spectroscopy, where the repetitive spark is formed in air or a carrier gas by a focused laser beam. This technique, capable of detecting aerosols directly in ambient air, is called LIBS which stands for laser-induced breakdown spectroscopy. The time integrated and time-resolved versions (sometimes called TRE-LIBS) have been discussed briefly (7, 8). This paper describes the technique in detail, the nature of the plasma, the computation of its properties, and some analytical results which are compared with those from the conventional argon ICP. The applications for which LIBS is well suited will be noted.

Soon after the discovery of laser-induced breakdown (LIB) of gases in 1963 (9), many studies discussed the mechanisms of breakdown and energy deposition. One of the principal experimental tools was time-resolved spectroscopy (10). These studies concentrated for the most part on sparks in simple atmospheres such as hydrogen (10), helium (11, 12), and other pure gases (13, 14). The current understanding of laser-induced breakdown of gases is well summarized in a review by Raizer (15). The classic method for generating a laser spark

in a gas is to focus a 1-10-J laser pulse to a fluence greater than 10 MW/cm<sup>2</sup> (15). Breakdown occurs because the electric field at the focus exceeds the dielectric strength of air, not because of selective absorption by an atom or molecule. However, selective absorption can reduce the breakdown threshold (16), which is otherwise a slowly varying function of wavelength. At atmospheric pressure, a cascade ionization develops when a few seed electrons absorb energy from the laser beam by inverse brehmsstrahlung (15). The plasma becomes opaque, absorbs more laser energy, and grows toward the focusing lens during the laser pulse. The result is a luminous plasma with a temperature of 10<sup>4</sup> to 10<sup>5</sup> K, and an electron density of 10<sup>15</sup> to 10<sup>19</sup> cm<sup>-3</sup>. By comparison, conventional arcs have temperatures in the 5000 to 7000 K range and electron densities of 10<sup>15</sup> cm<sup>-3</sup> (ref. 1, p 128 ff). High voltage sparks have temperatures of 10000 to 60000 K (17). The ICP generates temperatures of 6000 to 10000 K and electron densities of 10<sup>11</sup> to 10<sup>16</sup> cm<sup>-3</sup> (4). Local thermodynamic equilibrium (LTE) is not complete in any of the plasma sources mentioned above (18).

Spectrochemical applications of laser-induced breakdown took the direction of the laser microprobe technique in which the laser was the atomizing source (19). Spectra from vaporized surface material were generated by following the laser pulse with conventional spark excitation. These spectra were sharper and stronger than those produced by the laser alone (20). An instrument was constructed and marketed embodying these principles (21, 22). It was successful in determining relative concentrations of impurities in steels and alloys at the 10 to 1000 ppm level. Typical absolute limits of detection were 1 to 30  $\mu$ g (22). The technique has remained primarily a research tool for specialized applications.

When called upon to monitor beryllium directly in air; and to analyze the effluent stream of a coal gasifier, the authors reinvestigated the repetitive, electrodeless, laser-induced spark. This paper discusses the results of that investigation.

## EXPERIMENTAL SECTION

**Photomultiplier Detection.** The basic LIBS apparatus with time resolution is shown schematically in Figure 1. The components of the apparatus and the typical experimental conditions are listed in Table I. A 5- to 20-cm focal length lens focused the laser beam, pulsed at 10 Hz, to fluences which were sufficient to breakdown the carrier gas, typically 10<sup>8</sup> to 10<sup>9</sup> W/cm<sup>2</sup>. These fluence levels correspond to a field strength of  $2 \times 10^6$  V/cm, well in excess of that needed to cause a breakdown in air with a conventional spark. Gas pressures ranged from 100 to 760 torr, although most experiments were performed in air at Los Alamos atmospheric pressure of 580 torr.

Light from the plasma was collected and imaged on the slit of a scanning spectrometer. For detectors we used a variety of photomultiplier tubes with extended ultraviolet or red responses. The photomultiplier output was processed by a boxcar averager for time resolution and signal averaging. The delay between the plasma initiation and the time of observation ( $t_d$ ) was 0.2 to 20  $\mu$ s with 100-ns to 1- $\mu$ s windows. Time resolution was necessary to discriminate against the strong continuum emission at early times (<500 ns). The spectrometer was scanned slowly so that the signal peaks were not attenuated by the time constant of the electronics.

Table I. Experiment Apparatus and Settings Used for Laser-Induced Breakdown Experiments

<b>A. Laser</b>	
laser	Quanta-Ray DCR Nd:YAG
pulse width	10 ns
energy	100-300 mJ/pulse
wavelength	1064 nm
repetition rate	10 Hz
<b>B. Detection System</b>	
1. spectrometer	Spex Industries 0.5-m Czerny-Turner
grating	1200 or 3600 lines/mm
slit width	10-250 $\mu$ m
slit height	2 cm
2. photomultiplier tubes	RCA C31034, 1500-2000 V, Hamamatsu R955, 800-1200 V, thermoelectric cooling
3. photomultiplier signal processing	
a. boxcar averager	PAR 162 (Princeton Applied Research)
aperture delay	1-10 $\mu$ s
aperture duration	100 ns-1 $\mu$ s
trigger	external, from laser Q-switch output + slope, + level
b. gated integrator	PAR 164 (Princeton Applied Research)
input	50 $\Omega$ , dc
time constant	1, 10, or 100 $\mu$ s
averaging mode	exponential
4. chart recorder	Hewlett-Packard 7132A
speed	1-2 in./min
span	50 mV-10 V
5. diode array signal processing	
a. optical multichannel analyzer	Tracor-Northern/DARSS
d:ode array	1024 diodes in 2.54 cm
b. master p:user	Hewlett-Packard 8005B
c. delay generator	Nanofast 568-702
d. diode array gate p:user	PAR/EGG Model 1211
<b>C. Sampling</b>	
nebulizer	RETEC
takeup rate	0.17-0.25 mL/min
carrier gas flow rate	9-11 L/min
heat chamber temperature	<100 °C
solution concentration	40 ng/mL to 1 $\mu$ g/mL

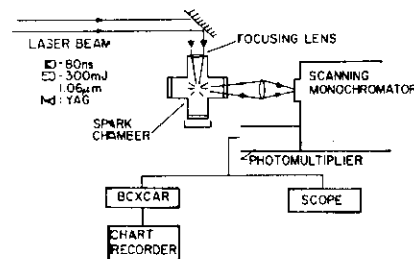


Figure 1. Schematic of the photomultiplier-boxcar arrangement for obtaining LIBS with time resolution.

Observation with the photomultiplier and spectrometer gave the maximum sensitivity over the range 200-900 nm. By contrast, the diode array detection scheme discussed below provided simultaneous monitoring over a wide spectral range, particularly useful for survey work not requiring maximum sensitivity.

**Detection via the Time-Gated Diode Array.** In another variation of the detection technique, we used a time-gated linear diode array coupled to a multichannel analyzer (MCA). The array consisted of 1024 diodes in 2.54 cm. Each channel of the MCA recorded the signal seen by one diode during each shot. If not gated, the diodes integrated all the incident energy. Often, the light imaging on the array went through a microchannel plate image intensifier, which can have a gain of 25000. With this combination the array was time-gated simply by switching on the high voltage to the intensifier during the time of interest, typically 200 ns to several microseconds. The schematic of Figure 2 shows such a time-gated intensified-array detector apparatus. This system was sensitive to wavelengths between 350 and 800 nm.

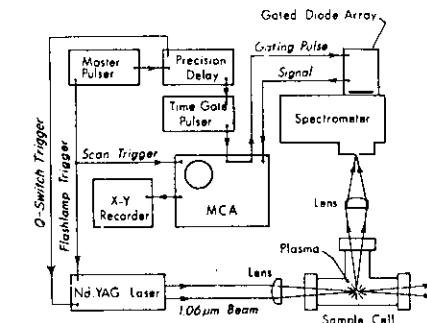


Figure 2. A schematic of the time-gated diode array system for providing time-resolution with LIBS.

**The Sampling Procedure.** Usually sample chambers were six-armed crosses, with the laser beam directed at right angles to the flowing sample and the direction of observation perpendicular to both. The focusing lens was mounted either independently of the chamber or immediately inside the chamber window. The unabsorbed part of the beam was allowed to exit freely from the cell. If it hit a surface close to the plasma, material ablated into the chamber introduced unwanted spectra and spark instability.

Beryllium particles (estimated diameter less than 10  $\mu$ m) were generated by laser ablation, and beryllium-chloride aerosol was produced by a nebulizer/heat-chamber system, similar to that described in ref 23. Other aerosols were generated only by the nebulizer/heat-chamber method. In laser ablation, the laser beam

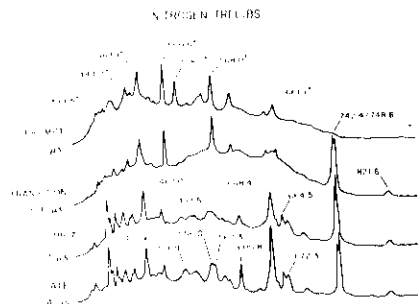


Figure 3. Time-resolved spectra of nitrogen taken with the diode array system. Note the dominance of continuum and ionic lines at early time, and the strength of the neutral lines at late time. The spectra have not been normalized and are only qualitative.

grazed a beryllium block and ablated a small amount of beryllium particulate on each shot. These small particles were then swept into the spark chamber where they were excited by the remainder of the beam. The size was estimated by capturing the particles on Millipore filters (pore size 0.8  $\mu\text{m}$ ) and looking at the filters with optical and electron microscopes. In the nebulizer/heat-chamber system, an aqueous beryllium solution of known concentration was aspirated into a pipe kept at a temperature above 100 °C and mixed with a flowing stream of air. This produced an aerosol of beryllium chloride. A nozzle at the end of the pipe directed the sample into the spark volume. The spark was not visibly affected by air flows of up to 10 L/min nor could we detect a variation in excitation conditions with air flow. Solution samples are not in general required for LIBS. The beryllium solution was simply a convenient method for introducing the particulate and changing its concentration in the sample chamber.

The commercially available nebulizer (see Table I) was one in which the condensate drained back into the reservoir and was again available for nebulization. Hence, the net uptake rate was the net change in fluid mass in the reservoir divided by the elapsed time. Very little sample was lost to the walls of the heat pipe. In one experiment, we recorded the amount of beryllium which passed through the heat pipe and then rinsed the pipe with hydrochloric acid. The resultant solution was analyzed for beryllium by atomic absorption. Less than 0.1% of the beryllium which passed through the system was found in the solution.

## RESULTS AND DISCUSSION

**Temporal Emission Characteristics.** The emission characteristics of the plasma varied with time as illustrated in Figure 3. Shortly after plasma initiation, the dominant radiation was a continuum mixed with ionic lines. Between 0.1 and 1  $\mu\text{s}$ , both of these contributions decayed, leaving neutral emission lines which were seen out to 20  $\mu\text{s}$  or longer. At intermediate and late times (>5  $\mu\text{s}$ ) molecular features also were present. We generally monitored in the quiescent time period between 1 and 20  $\mu\text{s}$  when background emission was reduced and the neutral lines remained intense. Ion lines were also used for analysis, but normally they were observed at early times,  $t_d < 0.5 \mu\text{s}$ . The Be II doublet at 313.1 nm was a significant long-lived exception, having been observed to 20  $\mu\text{s}$  and longer. The long lifetime was probably due to the high spark temperature, low excitation energy of the upper atomic level, and the large  $g_f$  value of the doublet which is isoelectronic with Li I. We have treated each spark as a separate entity uninfluenced by the preceding spark. However, the breakdown threshold was lowered slightly when operating at the usual repetition rate of 10 Hz.

**Spatial Profile.** To understand the shape of the plasma and of the energy deposition therein, we studied the plasma volume as a function of incident laser energy. The volume was determined by monitoring the continuum emission (314

## APPROXIMATE PLASMA SIZE VS ABSORBED LASER ENERGY

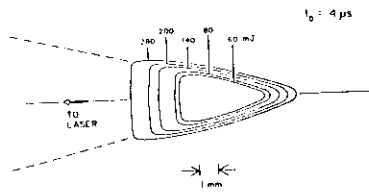


Figure 4. Plasma size in cross section at  $t_d = 4 \mu\text{s}$  and various laser energies. Dimensions were obtained by observing the spatial variation in the continuum at 314 nm.

nm,  $t_d = 4 \mu\text{s}$ ) as the plasma was scanned across the slit of the spectrometer by moving the imaging lens. The size of the plasma was taken as the distance between the  $e^-$  (13%) intensity points. We scanned both parallel to and perpendicular to the long axis of the plasma. An averaged intensity was recorded because the plasma is conical in shape and we only observed through the cone. Combining the measurements with visual observations we obtained the approximate dimensions and shape of the plasma shown in Figure 4.

**Energy Deposition.** To determine the energy deposited in the air plasma, we measured the transmission of the laser beam through the plasma. The energy transmitted varied from 20% at 70 mJ incident to 5% at 300 mJ incident. We could not detect any reflected laser energy. Since energy absorption is reportedly much lower in a helium plasma (11, 12), we also measured the latter. In helium the absorption was 19% at 64 mJ incident and 30% at 208 mJ incident, in reasonable agreement with reported values.

**Temperature and Electron Density.** Plasma temperatures are often determined from the ratios of intensities of ion to neutral lines and neutral to neutral lines, usually of the same element (24–26). These intensities are combined with the Saha equation and the electron density or with the Boltzmann equation to determine temperatures of the ionization equilibrium (sometimes called ionization temperature) and excitation temperature, respectively. Agreement between ionization and excitation temperature is a necessary but not a sufficient condition for LTE. Use of the Saha equation requires knowledge of the electron density, which we measured from Stark widths of the spectral lines as discussed below. We used C II/C I, N II/N I, and Be II/Be I intensity ratios for the ionization temperature and Be I lines for the excitation temperature. The term temperature is used in the discussion below because there is evidence for LTE after 1  $\mu\text{s}$  in the laser spark.

If the source is not spatially resolved the resultant temperature is a population-averaged temperature as discussed by Boumans (ref 25, p 149), a parameter which describes the source but is not identical with the temperature of each layer of the source. In one case we spatially unfolded the plasma emission via Abel inversion and determined temperatures which were less than 5% higher than population averaged temperatures. All other temperature measurements were made without unfolding and are population-averaged temperatures. Considering the uncertainties introduced by unfolding a small source of only approximate cylindrical symmetry, it was not clear that further effort on unfolding would improve the temperature or electron density values. Precise measurements of intensities and line widths will have to be made with high spatial resolution to accurately profile the temperature and electron density.

Under the assumption of LTE, temperatures have been calculated as described above. The results, as a function of

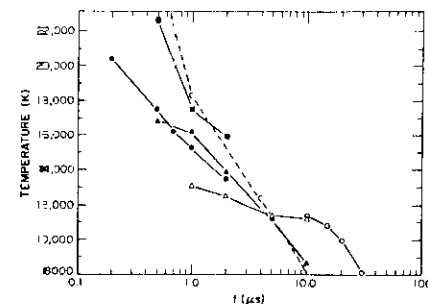


Figure 5. The temperature in an air plasma as a function of time. The ambient pressure was 580 torr. The various symbols refer to species and methods used in obtaining the temperatures: (●) C II 251.2/C I 247.8 nm; (■) N II 399.5/N I 415.0 nm; (○) Be II 313.0/Be I 234.8 nm; (▲) Be I Boltzmann plot; (Δ) Be II 313.0/Be I 234.8 nm spatially resolved by Abel inversion; C, calculated from hydrodynamic code.

time after spark initiation, are shown in Figure 5. At 1  $\mu\text{s}$  we find  $T = 15600 \pm 1800 \text{ K}$ , at 10  $\mu\text{s}$   $T = 10800 \pm 1400 \text{ K}$ , and at 30  $\mu\text{s}$   $T = 8100 \text{ K}$ . To measure temperatures by these methods it is important that the plasma be optically thin. We verified that the plasma was optically thin at the N I triplet, 414.3, 414.5, and 415.1 nm, which should have the intensity ratio of 1:2:3. The observed intensity ratio was within 10% of that predicted by the statistical weights of the upper levels.

Several lines of reasoning indicated that LTE existed at least after  $t_d = 1 \mu\text{s}$ . First, after  $t_d = 1 \mu\text{s}$ , the Be I excitation temperature agrees with the Be II/Be I ionization temperature to better than 20%. The beryllium was at such low concentrations that the plasma was dominated by the oxygen and nitrogen excitation. Second, the temperatures calculated on an LTE model, as discussed below, also fell among the analytically derived values, although the computed values were higher at early times and fell off more quickly at late times. Third, our temperature and electron density values at specific times agree with those calculated by using an equilibrium thermodynamic model of a low temperature air plasma (27), as illustrated in Figure 6. Fourth, Lochte-Holtgreven presents equations for calculating the time to establish electron-heavy particle LTE for a transient plasma. The theory is based upon particle density and collision frequency, which are both high in the atmospheric pressure LIB plasma. By use of our measured values at  $t_d = 1 \mu\text{s}$ , the time to establish such an equilibrium is calculated to be less than 20 ns, implying that LTE had already been established. The time to establish a Boltzmann population distribution is calculated to be much shorter. Finally, a recent work on LIB plasmas in nitrogen and oxygen (28) at 1.5 atm concluded that singly ionized oxygen atoms are in local thermodynamic equilibrium with the electrons at 15–20 ns into the LIBS discharge. Their conditions were not significantly different from those in the plasma under discussion. The present results are consistent with earlier spectroscopic temperature measurements of Mandelshtam et al. (29). Our conclusion is that the LIBS plasma behaves as if it were at, or very close to, a condition of LTE at times greater than 1  $\mu\text{s}$ .

Stark broadening is the major contributor to spectral line width for many species in the LIB plasma, especially at early times. Pressure broadening by neutral perturbers in LIB plasmas generally yields a detectable contribution only if the neutral particle density is greater than the charged particle density by a factor of  $10^3$  (ref 26, p 120), which in the LIB plasma occurs after 10  $\mu\text{s}$ . Even though temperatures are higher at early time and pressure broadening due to neutrals

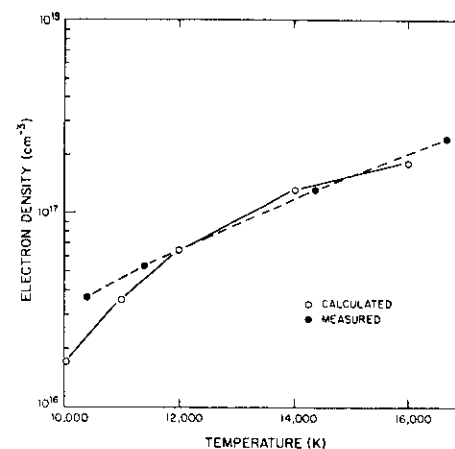


Figure 6. Comparison of measured electron density and temperature in LIBS with computations from an equilibrium model of a low temperature air plasma (27).

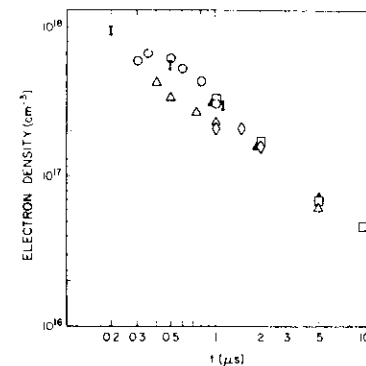


Figure 7. The electron density of an air plasma as a function of time. Ambient pressure was 580 torr. The lines used were (○) F I 685.8 nm; (Δ) Ar I 706.7 nm; (□ and ▲) N I 415.0 nm; (I) for N II 343.7, N II 395.5 and N II 399.5 nm; (●) Cl I, 837.5 nm.

is greater, the electron and ion concentrations are also higher. As a result, at all but late times the Stark broadening dominates. Doppler width is also insignificant in most cases. At one extreme, the Doppler width of N I 415 nm at 0.5  $\mu\text{s}$  is 0.01 nm, while the Stark width is 0.76 nm. At later times the Stark width is smaller, but always exceeds the Doppler width for N I 415 nm. At the other extreme, for Be II 313 nm the Stark broadening coefficients are small enough that Doppler width and pressure broadening by neutrals are the main contributors to line width. Usually the lines we observe have widths, corrected for instrumental width, between 0.1 and 0.3 nm.

Electron densities were determined from the Stark widths of various lines using the theory developed by Griem (24, 30) and elucidated by Lochte-Holtgreven (26). Observed line widths were corrected for the instrumental line width. The results are shown in Figure 7. The electron density in the spark was  $9 \times 10^{17} \text{ cm}^{-3}$  from ion lines at early time and  $5 \times 10^{16} \text{ cm}^{-3}$  from neutral lines at late time. Much of the scatter in the curves is due to the limitation in the accuracy of the theory. Reference 30 quotes that accuracy as 25–30% for



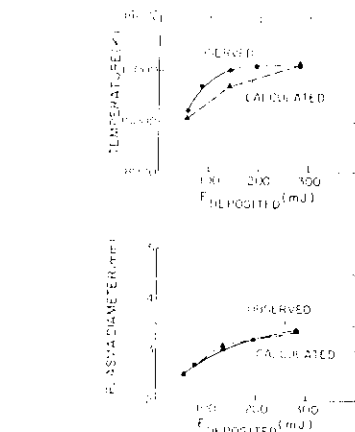


Figure 8. Computed and measured temperature and plasma diameter as a function of energy deposited at  $t_d$  of 4  $\mu$ s. Temperature was measured from the ratios of intensities of Be II 313 nm to Be I 235 nm.

neutral lines and 50% for ion lines. The electron densities from the ion lines were reduced by a factor of 3, as suggested in ref 30. The LIB electron densities are high compared to arcs (1) and ICP (4).

**Modeling.** We have used a one-dimensional radiation-coupled-hydrodynamics code (37) to model the temporal behavior of the laser-heated air plasma. The code numerically integrates the partial differential equations that describe the conservation of mass, momentum, and energy of the air, in the presence of radiative energy transfer. The latter is treated in the diffusion approximation with a single frequency-averaged opacity. The opacity is a tabulated function of the temperature and density of the air, as is the pressure. We assume that the low level of contaminants has no effect on the hydrodynamic response of the air, or on radiative transfer. The spark is assumed to have one-dimensional cylindrical symmetry. The radial coordinate is the only spatial variable of interest. In order to bring the temperature into the right range we empirically varied a parameter analogous to emissivity called a "flux limiter". No attempt was made to find an a priori value for this parameter.

To simulate the effect of the laser pulse, internal energy was introduced into the innermost computational zone (of radius 0.001 cm) at a constant rate over 10 ns. The calculation used a linear energy density of deposition of 40 mJ/mm. The pressure was taken to be the Los Alamos atmospheric pressure. The energy heats the zone and raises its pressure, causing it to expand and decrease in density. Radiation and conduction meanwhile transport some of the energy into exterior zones, causing them likewise to heat and expand. From this model we calculated the temperature and air density as functions of radial position and  $t_d$ . The calculated temperature as a function of time is shown in Figure 5 along with the experimental values. The agreement is good, with the calculated values decaying slightly faster than the experimental. Figure 8 shows the calculated and observed dependence of the plasma diameter and temperature upon deposited laser energy, at  $t_d$  of 4  $\mu$ s. Considering the simplicity of the model, the agreement is striking. According to Figure 8, there is only about a 20% increase in spark temperature as the laser energy is increased 5-fold from 60 to 300 mJ/pulse. Evidently, over this energy range, additional laser energy is channeled into producing a larger plasma rather than changing some of the spark prop-

erties. The same value of the flux limiter was used for all calculations. With this simple model we will be able to predict plasma properties as a function of laser energy, ambient pressure, and other variables.

**Beryllium Detection.** We have applied LIBS to direct sampling of beryllium in air. It is a problem in environmental monitoring which has been previously approached by emission spectroscopy (32-34). For purposes of calibration and limit-of-detection measurements, we chose to generate beryllium in air via the nebulizer/heat-chamber apparatus. Net signals were obtained by scanning the spectrometer wavelength over the unresolved Be II doublet at 313.1 nm and subtracting the background from the signal. The signal-to-continuum ratio was then taken to compensate for drift in laser energy. Noise was determined by two methods: by measuring the root mean square (RMS) of the noise on the off-line background, and by calculating the RMS variation of the signals obtained on 16 scans of the Be II doublet. The two methods gave the same RMS noise. The beryllium concentration in air was calculated from

$$c_a = \frac{c_s \times \text{net uptake rate}}{\text{carrier gas mass flow rate}} \quad (1)$$

where  $c_s$  is the concentration in air ((w/w) analyte atom to air molecule),  $c_a$  is the solution concentration (ng/mL), the net uptake rate is in mL/min, and the mass flow rate is in g/min. A linear calibration curve was developed which covered the range of  $c_s$  from 0.5 to 5 ng/g. Since the calibration curve did not pass through the origin, we took the limit of detection ( $c_L$ ) as that concentration at which the net signal was three times the noise, a relative standard deviation (RSD) of 30%. This occurred at  $c_s = 0.6$  ng/g. The corresponding solution concentration was 40 ng/mL. At all other points on the calibration curve the RSD was 10%.

Representative solution limits of detection for beryllium in the ICP are 0.3 ng/mL when Be II 313.1 nm is used and 0.003 ng/mL for Be I 234.8 nm (35). To aid the reader in comparing LIBS and ICP detection limits, we have converted the ICP limits to aerosol concentrations via eq 1. Assuming a typical uptake rate of 1 mL/min of solution, and an argon analyte flow rate of 1 L/min, the ICP limit for the 313.1-nm line becomes 0.2 ng/g ((w/w) Be atom to Ar atom), which is 2.5 times lower than the LIBS limit determined in air.

The OSHA limit for average exposure to beryllium is 2  $\mu$ g/m<sup>3</sup>; the 1/2-h maximum permissible exposure is 25  $\mu$ g/m<sup>3</sup>. Our detection limit of 0.6 ng/g corresponds to 0.7  $\mu$ g/m<sup>3</sup>. It is a useful limit, and one that can be realized in real time, in contrast with the atomic absorption beryllium detection method which is slowed by sample preparation time.

**Limits of Detection: Other Elements.** The same nebulizer/heat-chamber apparatus was used to establish limits of detection for other elements directly in air. In each case standard solutions were diluted, nebulized, and passed through the heat chamber into the sample chamber. Table II lists the elements, analytical lines, the time delay employed, the limit of detection determined as for beryllium, and a corresponding limit of detection for ICP. The comparison to ICP is not straightforward. We did not optimize our experiments for low solution concentrations since we were interested in detecting elements directly in air. Units of ng/g (analyte atom to air molecules) were appropriate for LIBS. As in the case of beryllium, we have converted the ICP solution detection limits (35) to ng/g (analyte atom to argon atom) via eq 1, assuming solution uptake rate of 1 mL/min and an argon flow rate of 1 L/min. The aerosol limits of detection for ICP are quoted in the last column of Table II. Uniformly, the limits of detection for the ICP using argon are lower than those for LIBS directly in air.

Table II. Limits of Detection for Some Elements in LIBS and ICP<sup>a</sup>

species	analytical line, nm	$t_d$ , $\mu$ s	$c_L$ (LIBS) <sup>b</sup> , $\mu$ g/g	$c_L$ (ICP) <sup>c</sup> , $\mu$ g/g
Be II	313.1	4	0.0006	0.0002
Na I	588.9	4	0.006	0.00006
P I	253.3	2	1.2	0.015
As I	228.8	2	0.5	0.004
Hg I	253.6	2	0.5	0.0006

<sup>a</sup> Reference 35. <sup>b</sup> The  $\mu$ g/g refers to  $\mu$ g of analyte atom to gram of air molecule. <sup>c</sup>  $c_L$  means limit of detection.

<sup>c</sup> The  $\mu$ g/g refers to  $\mu$ g of analyte atom to gram of argon atom. To convert from the solution concentrations given in ref 35, we assumed a takeup rate of 1 mL/min and an argon flow rate of 1 L/min.

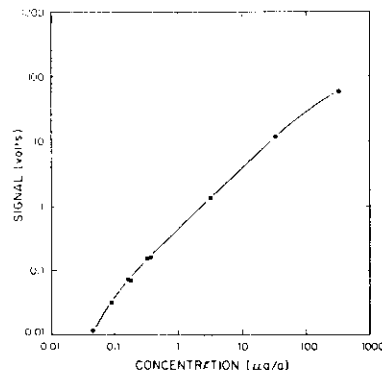


Figure 9. Calibration curve for sodium in air. Concentration units are (w/w) sodium atom to air molecule.

**Precision and Linearity.** To test the linearity of LIBS, a calibration curve for sodium was generated which covered nearly 4 orders of magnitude. It is shown in Figure 9. The solution concentrations varied from 5 to 10000  $\mu$ g/mL corresponding to airborne concentrations of 46 ng/g to 339  $\mu$ g/g (Na atom to air molecule). The RSD on all points was less than 10%. The region from 165 ng/g to 33  $\mu$ g/g is fit on a log-log plot by a straight line with a slope close to one. The curve began to level out at the highest concentration, possibly due to self-absorption, or perturbation of the plasma by the high sodium concentration. In ICP, RSD is usually less than 2%, and the calibration curve is often linear over 4 orders of magnitude (4).

**Field Experiments.** One of the advantages of LIBS is that it can be employed in field situations to interrogate samples directly in situ, and in real time. For in situ operations in the Los Alamos beryllium shop, the laser, focusing optics, spark chamber, electronics, spectrometer, vacuum pump, and chart recorder were mounted on a movable table. Ambient air samples from the shop were drawn into the chamber by the vacuum pump through a funnel and a long Teflon tube. The signal was full of spikes as particles traversed the spark chamber. By observing the frequency of the spikes, we could always tell when the safety air was on or off. The overall sensitivity of the apparatus was low, because of the inefficient transport of the beryllium to the spark chamber. However, the principle of the method was demonstrated. For routine operation, an in situ calibration procedure needs to be devised.

In another field experiment, the apparatus, this time with the diode array as detector, was taken to the Brigham Young

University experimental coal gasifier (36). Two optical ports were placed into the pipe containing the effluent gas stream at a point beyond a cyclone separator which removed the bulk of the particles. The spark was generated directly in the pipe carrying the gasifier effluent. Spectra were recorded, both in real time with the diode array and by photographic methods, and the following species were detected: Na, K, H, O, O<sup>+</sup>, C, C<sup>+</sup>, Ca, Ca<sup>+</sup>, Si, Mg<sup>+</sup>, CN, N<sub>2</sub>, CO, O<sub>2</sub>. Recently the apparatus was taken to another experimental coal gasifier at the Morgantown Energy Technology Center, Morgantown, WV. There the spark was generated in a clean effluent stream carrying N<sub>2</sub>, H<sub>2</sub>, O<sub>2</sub>, and other gases at 10 atm and 100 °C. Real-time spectra of N, H, O, S, and Ar were observed. Variations in H and O concentrations over a period of minutes were monitored.

## CONCLUSION

LIBS is a promising technique for obtaining spectrochemical information from sample locations where it is difficult to place electrodes or extract samples. LIBS can also sample species directly in air or a carrier gas, eliminating sample preparation. A common disadvantage of direct sampling is the possible inhomogeneity of the sample, leading to higher RSD. Calibration also promises to be a problem in the real world. The wide lines will cause a greater number of spectral interferences in complex samples. However, where these disadvantages can be overcome, LIBS will allow monitoring of species in environments where conventional electrode or plasma sources cannot be placed, in air or other carrier gases. In the following paper we discuss the application of LIBS to detecting fluorine and chlorine in air (37).

## ACKNOWLEDGMENT

We gratefully acknowledge the technical assistance of Ron Martinez. Thomas Niemczyk (University of New Mexico) made many useful suggestions about the content and arrangement of this paper.

Registry No. Be, 7440-41-7; Na, 7440-23-5; P, 7723-14-0; As, 7440-38-2; Hg, 7439-97-6.

## LITERATURE CITED

- Boumans, P. W. J. M. In "Analytical Spectroscopy Series"; Grove, E. L., Ed.; Marcel Dekker: New York, 1972; Vol. 1, Part 2, Chapter 8.
- Walters, J. P. *Science* 1977, 196, 787-797.
- Vickers, T. J.; Winefordner, J. D. In "Analytical Spectroscopy Series"; Grove, E. L., Ed.; Marcel Dekker: New York, 1972; Vol. 1, Part 2, Ch. 7.
- Barnes, R. M. *CRC Crit. Rev. Anal. Chem.* 1978, 9, 203-296.
- Car, J. W.; Horlick, G. *Spectrochim. Acta, Part B* 1982, 37B, 1-15.
- Ishizuka, T.; Uemawo, Y. *Anal. Chem.* 1980, 52, 125-129.
- Loree, T. R.; Radziemski, L. J. *Plasma Chem. Plasma Proc.* 1981, 1, 271-280.
- Radziemski, L. J.; Loree, T. R. *Plasma Chem. Plasma Proc.* 1981, 1, 281-291.
- Maker, P. D.; Terhune, R. W.; Savage, C. M. "Quant. Elec. Proc. 3rd International Conf., Paris 1963. Grivet, P., Bloembergen, N., Eds.; Columbia University Press: New York, 1964; Vol. 2, pp 1559-1576.
- Livak, M. M.; Edwards, D. F. *IEEE J. Quantum Electron.* 1980, QE-2, 486.
- Braerman, W. F.; Stumpell, C. R.; Kunze, H.-J. *J. Appl. Phys.* 1969, 40, 2548-2554.
- George, E. V.; Bekefi, G.; Ya'akobi, B. *Phys. Fluids* 1971, 14, 2708-2713.
- Stevenson, R. W. "Spectroscopic Examination of Carbon Dioxide Laser Produced Gas Breakdown"; Thesis, Naval Postgraduate School, Monterey, CA, 1975.
- Allison, S. W. "Laser-Induced Emission from UF<sub>6</sub>"; Thesis, University of Virginia, Charlottesville, VA, 1979.
- Raizer, Y. P. "Laser-Induced Discharge Phenomena"; Consultants Bureau: New York, 1977.
- Zapka, W.; Tam, A. C. *J. Opt. Soc. Am.* 1981, 71, 1585.
- Kremp, H. Z. *Phys.* 1982, 167, 302-325.
- Margoshes, M. *Appl. Spectrosc.* 1987, 21, 92-99.
- Laque, K. In "Analytical Laser Spectroscopy"; Omenetto, N., Ed.; Wiley: New York, 1979; Chapter 2.
- Rasberry, S. D.; Scribner, B. F.; Margoshes, M. *Appl. Opt.* 1987, 26, 81-86.
- Brech, F.; Cross, L. *Appl. Spectrosc.* 1982, 76, 59.
- "Laser Microprobe Mark III"; Jarrell Ash Technical Bulletin No. 71, June 1976.

- (23) Veillon, C.; Murgoshes, M. *Spectrochim. Acta, Part B* **1988**, *23B*, 553-555.
- (24) Griem, H. R. "Plasma Spectroscopy"; McGraw-Hill: New York, 1964.
- (25) Boumans, P. W. J. M. "Spectrochemical Excitation"; Hilger & Watts Ltd.: London, 1968.
- (26) Lochte-Holtgreven, W. In "Plasma Diagnostics"; Lochte-Holtgreven, W., Ed.; North-Holland: Amsterdam, 1968; Chapter 3.
- (27) Dresvin, S. V., Ed. "Physics and Technology of Low-Temperature Plasmas"; English edition by The Iowa State University Press: Ames, IA, 1977; p 22.
- (28) Stricker, J.; Parker, J. G. J. *Appl. Phys.* **1982**, *53* (2), 851-855.
- (29) Mandelzhtam, S. L.; Pashinin, P. P.; Prokhorov, A. V.; Prokhorov, A. M.; Sukhodrov, N. K. *Zh. Eksp. Teor. Fiz.* **1984**, *47*, 2003-2005 (Sov. Phys. - JETP (Engl. Transl.) **1984**, *20*, 1344-1346).
- (30) Griem, H. R. "Spectral Line Broadening by Plasmas"; Academic Press: New York, 1974.
- (31) Cox, A. N.; Brownlee, R. R.; Eilers, D. D. *Astrophys. J.* **1966**, *144*, 1024-1037.
- (32) Churchill, W. L.; Gillieson, A. H. C. P. *Spectrochim. Acta* **1952**, *5*, 238-250.
- (33) Rozsa, J. T.; Stone, J.; Uguccini, O. W. *Appl. Spectrosc.* **1965**, *19*, 7-9.
- (34) Wobb, M. S. W. *Atom* **1980**, No. 45, 20-31.
- (35) Parsons, M. L.; Forster, A.; Anderson, D. "An Atlas of Spectral Interferences in ICP Spectroscopy"; Plenum Press: New York, 1980.
- (36) Loree, T. R.; Radziemski, L. J., Proc. 1981 Symp. Instr. and Control for Fossil Energy Prog., Argonne National Laboratory Press: Argonne, IL, 1982; ANL-81-62/Conf-810607, pp 768-774.
- (37) Cremers, D. A.; Radziemski, L. J. *Anal. Chem.*, following paper in this issue.

RECEIVED for review March 26, 1982. Resubmitted October 19, 1982. Accepted March 28, 1983. This work was performed under the auspices of the U.S. Department of Energy.

## Detection of Chlorine and Fluorine in Air by Laser-Induced Breakdown Spectrometry

David A. Cremers and Leon J. Radziemski\*

University of California, Los Alamos National Laboratory, Chemistry Division, Los Alamos, New Mexico 87545

The use of laser-induced breakdown spectrometry (LIBS) to spectrometrically detect chlorine and fluorine in air directly is investigated. A laser-generated spark is used to atomize chlorine- and fluorine-bearing molecules. The atoms are then electronically excited by the high temperatures of the spark. Emission from the neutral atoms is spectrally and temporally resolved to maximize the signal-to-noise ratio. Optimization of the time window and laser power for minimum detection limits is discussed. The use of LIBS to determine the ratios of the numbers of different types of atoms on a molecule is considered. Minimum detectable concentrations of chlorine and fluorine in air are 8 and 38 ppm (w/w), respectively. Minimum detectable masses of chlorine and fluorine are, respectively, 80 ng and 2000 ng in air and 3 ng for both atoms in He. The precision for replicate sample analysis is 8% RSD.

Chlorine and fluorine atoms are difficult to detect by emission or absorption techniques because of the high-lying excited electronic energy levels. The resonance transitions of these elements lie in the vacuum-ultraviolet spectral region, below 140 nm for Cl and 100 nm for F. Detection capabilities in this region are limited by atmospheric and materials absorption, as well as detector sensitivity. The strong 837.6 nm Cl I and 685.6 nm F I excited-state transitions are more amenable to detection but have upper levels 10.40 and 14.50 eV, respectively, above the ground state. Plasma techniques characterized by high sample temperatures present good opportunities for detection using emission. The inductively coupled argon plasma (ICP) has attained detection limits for Cl and F in gas samples at levels of 50 and 350 ng, respectively (1, 2). The microwave-excited atmospheric pressure helium plasma (MEP) has detected as little as 0.016 ng/s of Cl and 0.0085 ng/s of F from the effluent of a gas chromatograph (3). In contrast to detection using these continuously operating plasmas, the ac spark between two electrodes represents another high temperature plasma suitable for excitation of Cl and F. Commercial instruments incorporating an ac spark can routinely monitor halogens in air at levels >1 ppm (4).

However, these devices are not element specific because they do not monitor the elemental emission lines directly but instead use some feature of the plasma which is perturbed by the presence of halogens.

The method of spark spectrometry is well established and has been used to detect a variety of elements. Recently, a variation of this technique has been developed which uses a focused laser pulse to generate the plasma (5, 6). This method, termed laser-induced breakdown spectrometry (LIBS), offers certain advantages over the older electrode-based techniques of spark spectrometry. For example, in the LIBS version there are no electrodes to wear or to introduce spectral interferences or perturbations of the plasma. In addition, the LIBS technique is noninvasive since only optical access is required to the sample to generate the laser spark. The question remains, however, whether LIBS can deliver these advantages and still produce useful detection limits. Because of the somewhat different properties of the LIBS plasma compared to other spark sources we present here a discussion of its characteristics in terms of Cl and F, two elements difficult to detect spectroscopically.

### EXPERIMENTAL SECTION

**Apparatus.** The LIBS apparatus for time-resolved spectral studies of the plasma by photomultiplier detection is described in detail in the previous paper (7). The experimental equipment and conditions used here are listed in Table I. Briefly, the air plasma was produced by focusing a Nd:YAG laser pulse. Emission from the plasma was spectrally resolved by a spectrometer and monitored with a photomultiplier tube (PMT). Signal processing and time resolution of the plasma light were provided by a boxcar averager.

**Procedure.** Fluorine- and chlorine-containing species were introduced into the air spark by using one of three methods: (1) gas mixtures, (2) liquid evaporation, or (3) pneumatic nebulization. Species that are gases at room temperature ( $\text{CCl}_2\text{F}_2$ ,  $\text{CClF}_3$ ,  $\text{SF}_6$ ) were premixed with air to 1000 ppm (v/v) in a large gas cylinder. These mixtures were then diluted with a carrier gas of air in a manifold connected to the spark chamber by 6 m of copper tubing. The length of the tubing was chosen to ensure thorough mixing of the carrier and sample containing gases. Flow rates of both gases were monitored to calculate the final concentrations of Cl or F bearing molecules in the spark chamber. Carrier gas flows